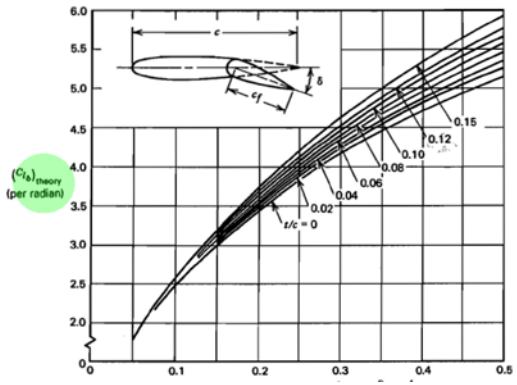

$$C_{L_{\delta_e}} \quad C_{M_{\delta_e}}$$

$$C_{N_{\delta_a}} \quad C_{L_{\delta_a}} \quad C_{Y_{\delta_a}}$$

$$C_{N_{\delta_r}} \quad C_{L_{\delta_r}} \quad C_{Y_{\delta_r}}$$

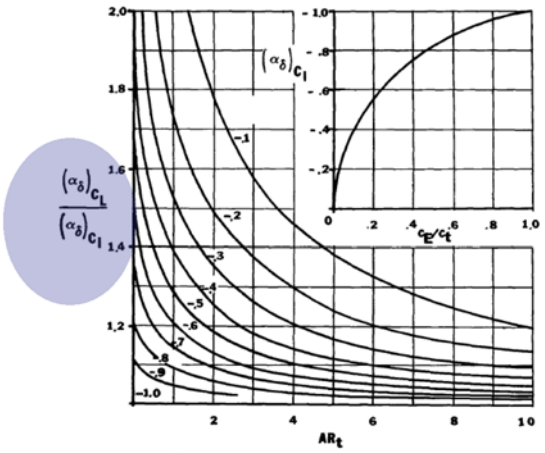

Figure 16. Flap chord factor.

Estabilidad y Control Detallado

Derivadas Estabilidad Control

Fig 31A

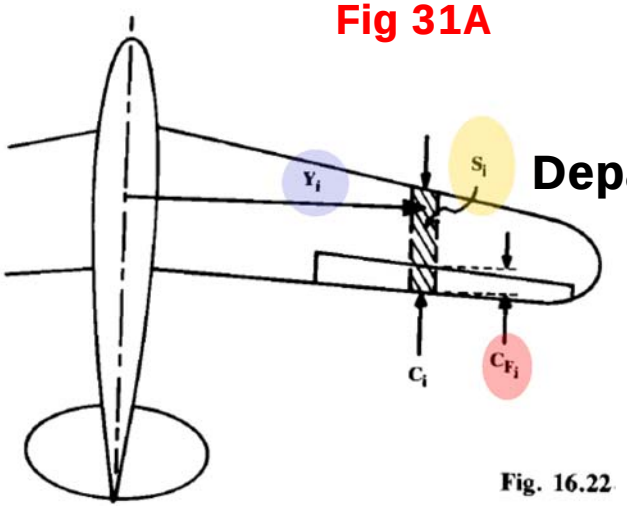

Fig. 16.22

Tema 14.4

Sergio Esteban Roncero
Departamento de Ingeniería Aeroespacial
Y Mecánica de Fluidos

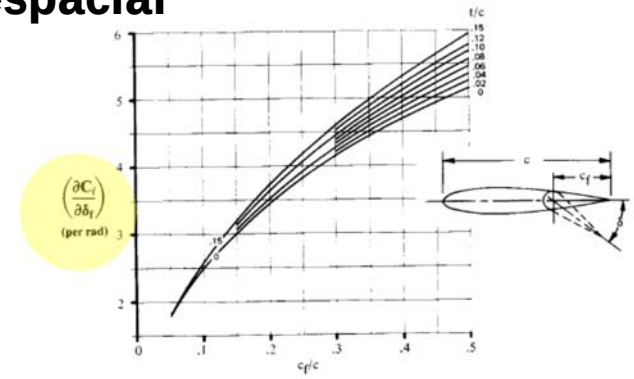

Fig. 16.6 Theoretical lift increment for plain flaps. (Ref. 37)

Control Derivatives $C_{L_{\delta_e}}$

Método I Simplificado

Método válido para: horizontal, canard

$$C_{L\delta_E} = \frac{dC_{L_t}}{d\alpha_t}\frac{d\alpha_t}{d\delta_E}$$ ⇒ $(dC_{L_t})/(d\alpha_t)$ = lift curve slope of the tail

$C_{L_{\delta_e}}$

Fig A34

Relación entre la superficie de control (S_E) y la superficie aerodinámica (S_t)

Cannard o Horizontal móvil $S_E/S_t = 1$ (extrapolación)

Fig A34

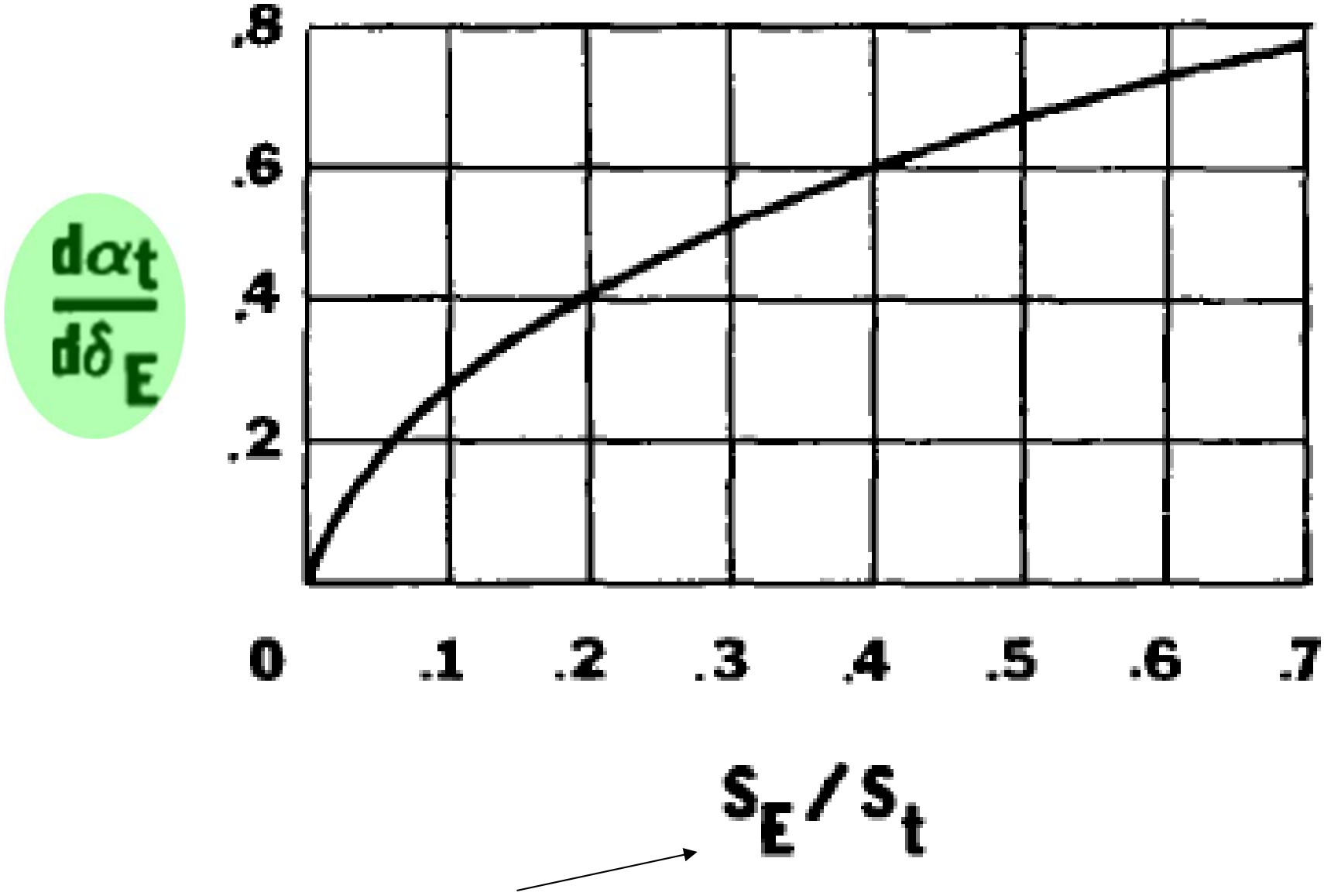

Relación entre la superficie de control (S_E) y la superficie aerodinámica (S_t)

Control Derivatives $C_{L_{\delta_e}}$

Método II

$C_{L_{\delta_e}}$ The change in lift coefficient due to elevator deflection

$C_{L\alpha}$ corregido 3D

$$C_{L\delta_E} = C_{\ell\delta_E} \left(\frac{C_{L\alpha_t}}{C_{\ell\alpha_t}}\right) \left(\frac{(\alpha_\delta)_{C_L}}{(\alpha_\delta)_{C_\ell}}\right) K_b$$

$C_{L\alpha}$ 2D

$C_{\ell\delta_E}$ = section lift curve increment due to flap (elevator) deflection (this derivative should not be confused with the rolling moment coefficient appearing in the lateral dynamics).

$C_{L\alpha_t}$ = lift curve slope of tail without flap deflected (3-D)

$C_{\ell\alpha_t}$ = section lift curve slope of basic airfoil

$\frac{(\alpha_\delta)_{C_L}}{(\alpha_\delta)_{C_\ell}}$ = ratio of 3-D flap effective parameter to the 2-D flap effectiveness parameter obtained from the figure below as a function of wing (tail) aspect ratio and the theoretical value of $(\alpha_\delta)_{C_\ell}$. The theoretical value is also given as a function of flap chord to airfoil chord.

K_b = flap-span factor which is ≈ 1.0 for elevator horizontal tail surface for light airplanes.

Fig A35

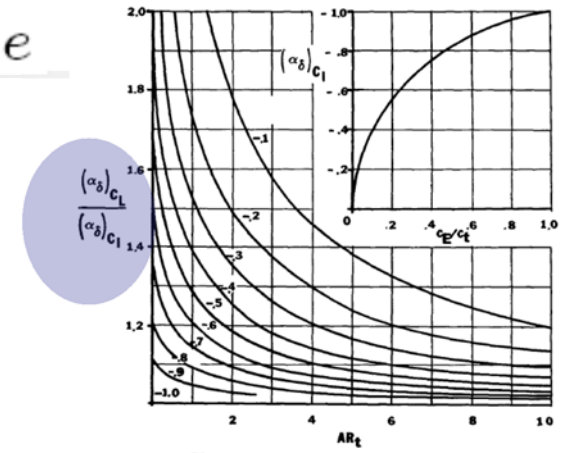

Figure 16. Flap chord factor.

Fig A36

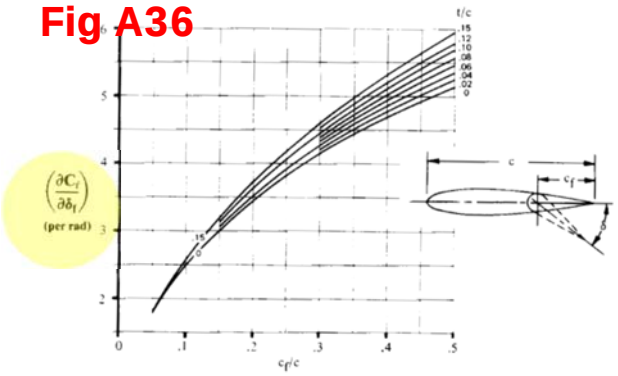

Fig. 16.6 Theoretical lift increment for plain flaps. (Ref. 37)

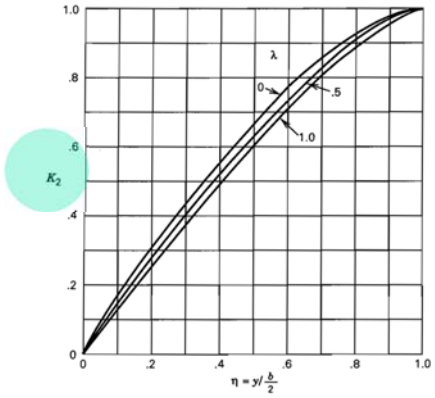

Figure B.2,3 Span factor for inboard flaps.

Fig A37

Fig A35

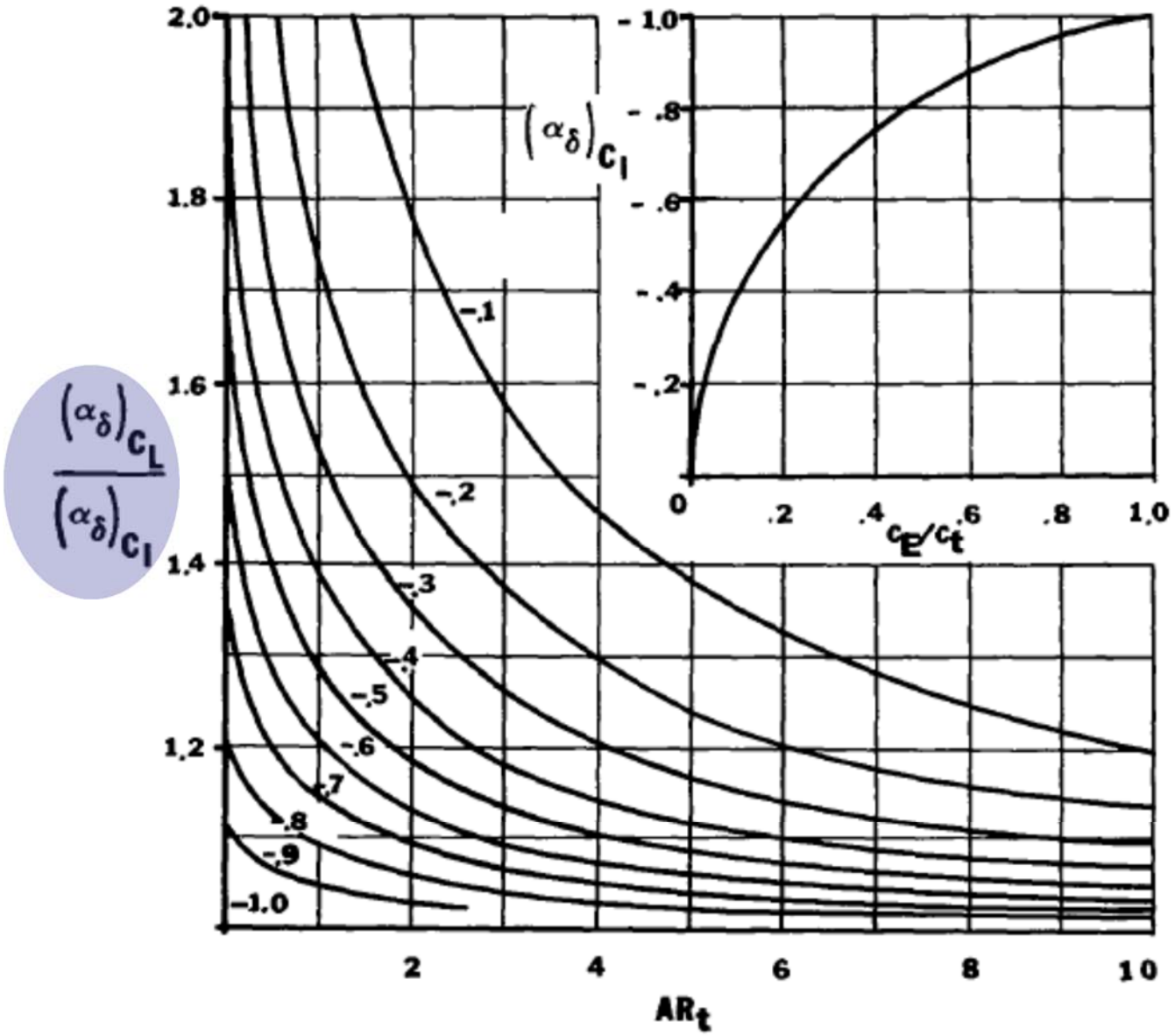

Figure 16. Flap chord factor.

Fig A35

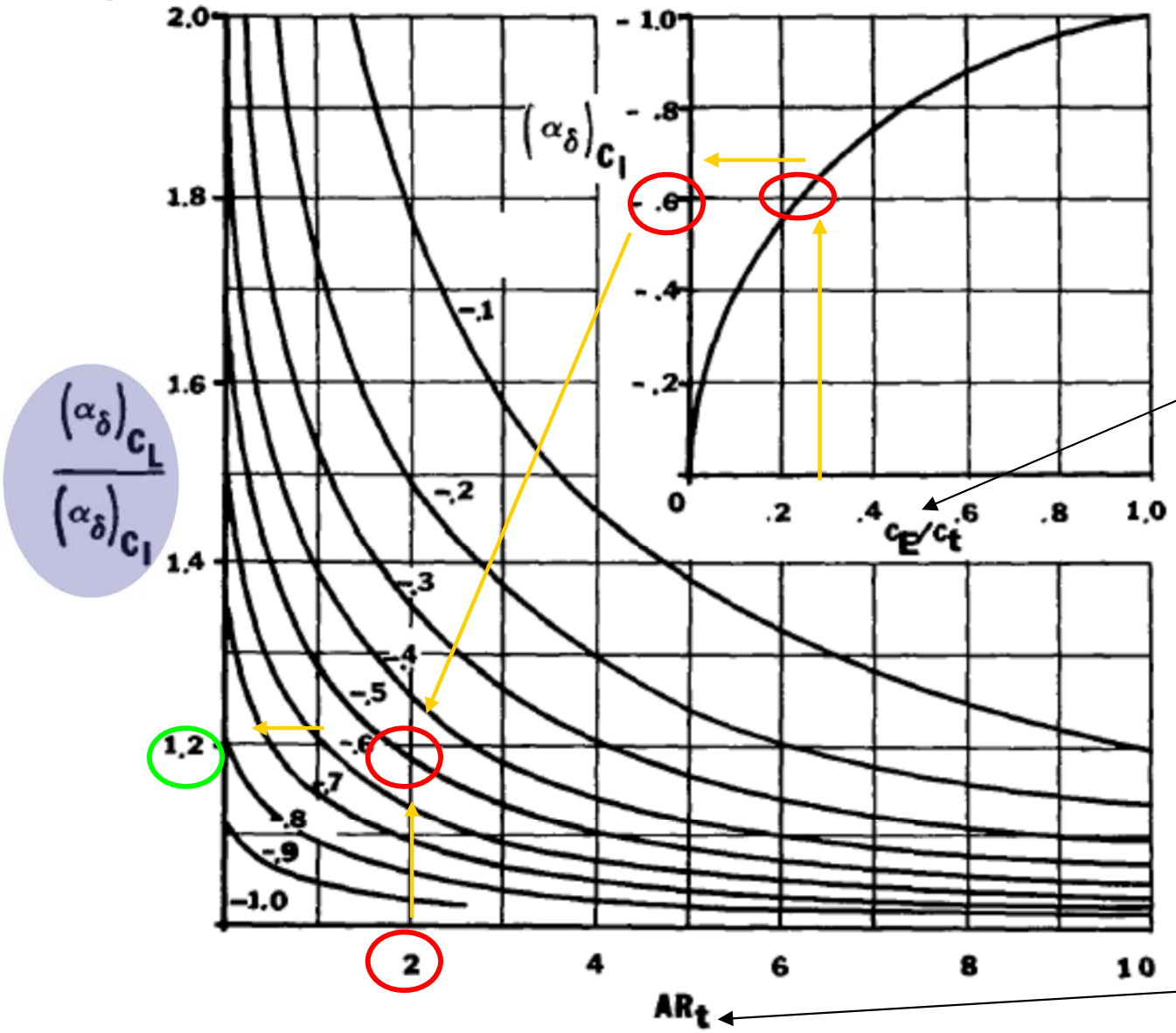

Figure 16. Flap chord factor.

Relación entre cuerdas superficie de control/ estabilizador

- Selección c_E/c_t
- Genera $(\alpha_\delta)_{Cl}$
- Selección AR_t y $(\alpha_\delta)_{Cl}$

-Genera $(\alpha_\delta)_{CL}$ $(\alpha_\delta)_{Cl}$

Alargamiento del estabilizador

Fig A36

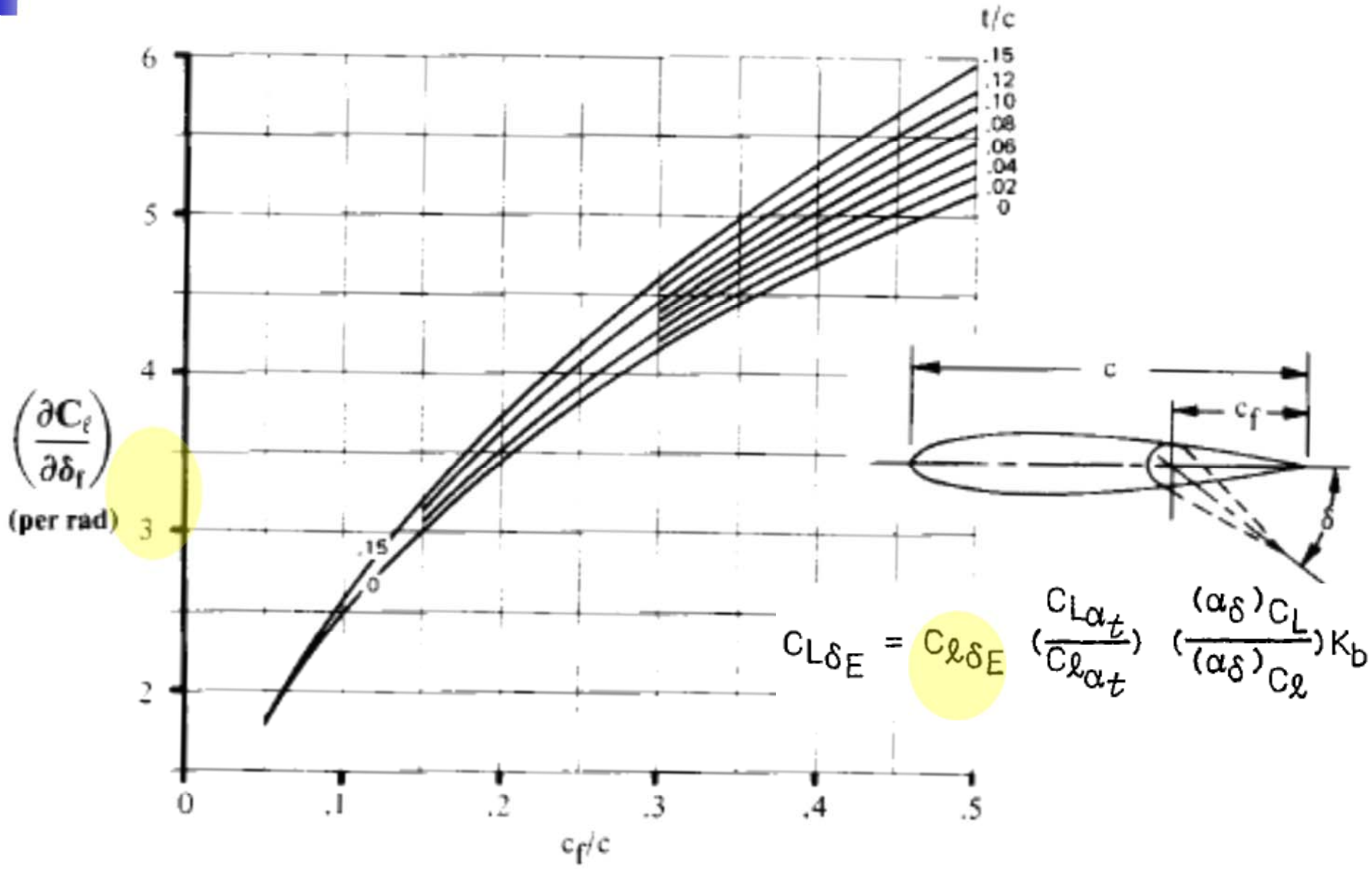

Fig. 16.6 Theoretical lift increment for plain flaps. (Ref. 37)

Fig A31I

$$C_{L\delta_E} = C_{\ell\delta_E} \left(\frac{C_{L\alpha_t}}{C_{\ell\alpha_t}}\right) \left(\frac{(\alpha_\delta)_{C_L}}{(\alpha_\delta)_{C_\ell}}\right) K_b$$

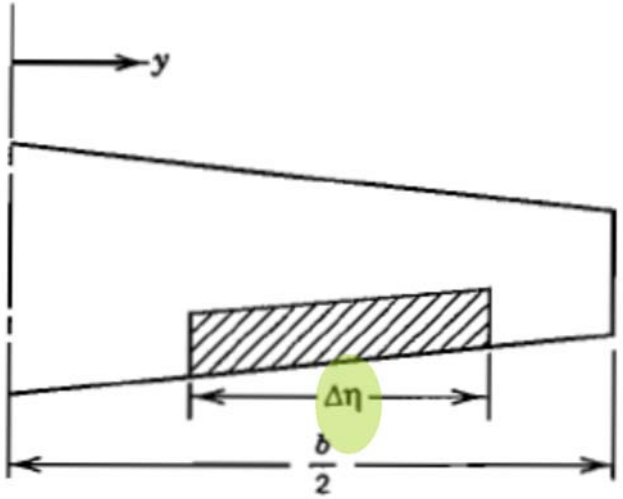

$K_b = K_2$

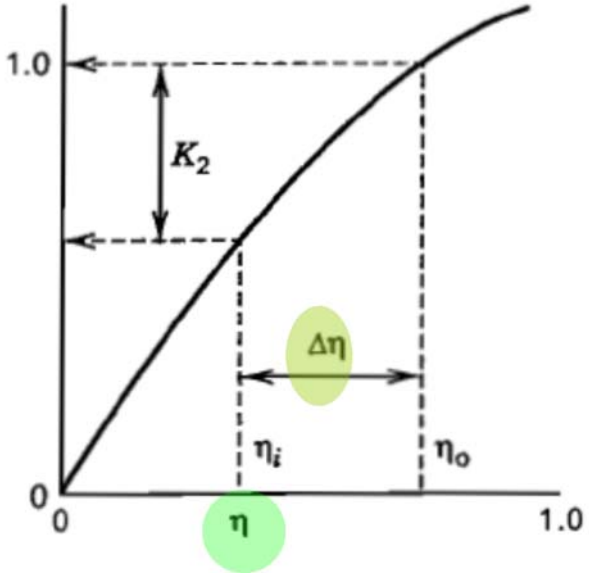

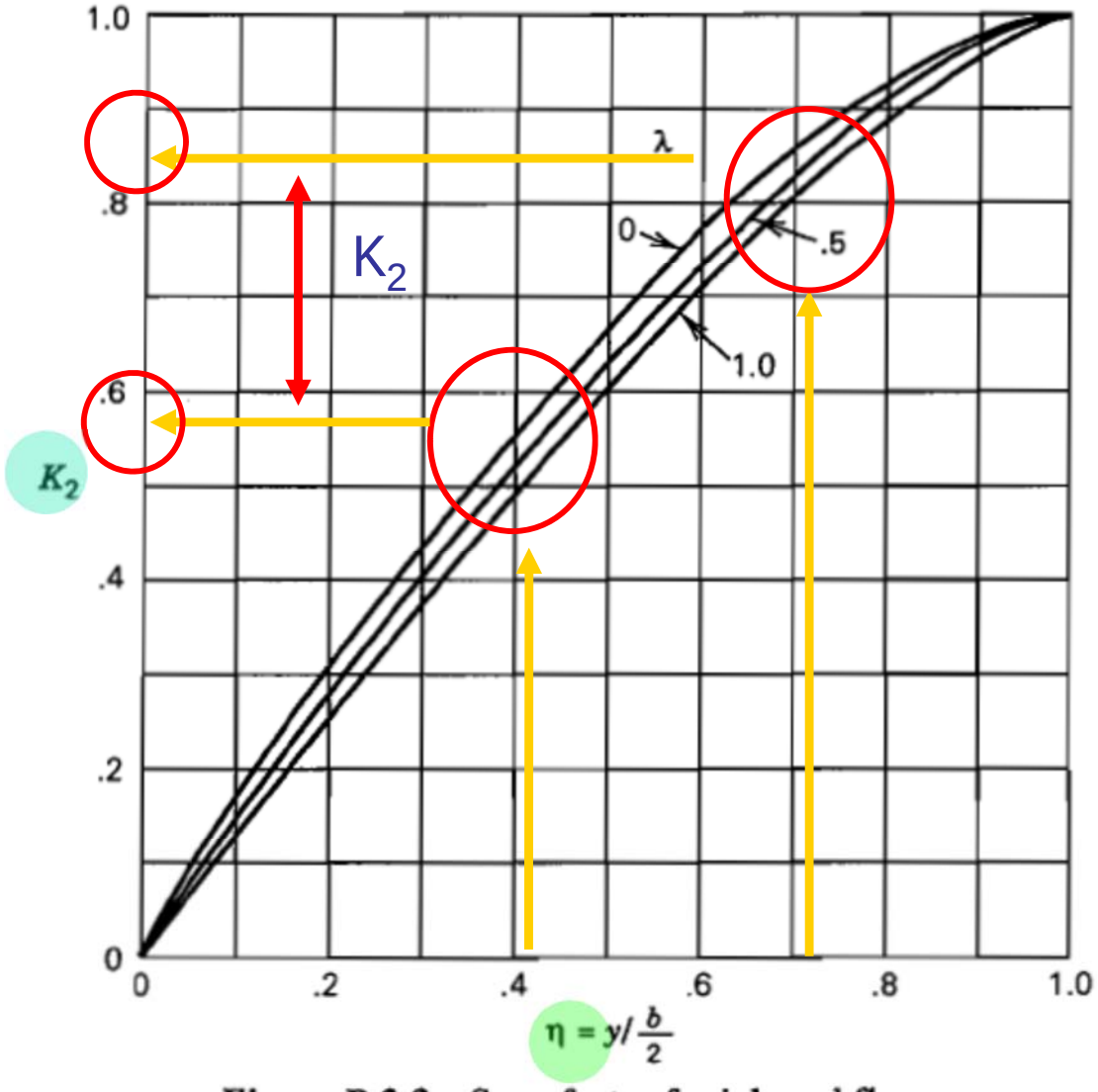

Figure B.2,3 Span factor for inboard flaps.

Efectividad de las superficies de control

Método III

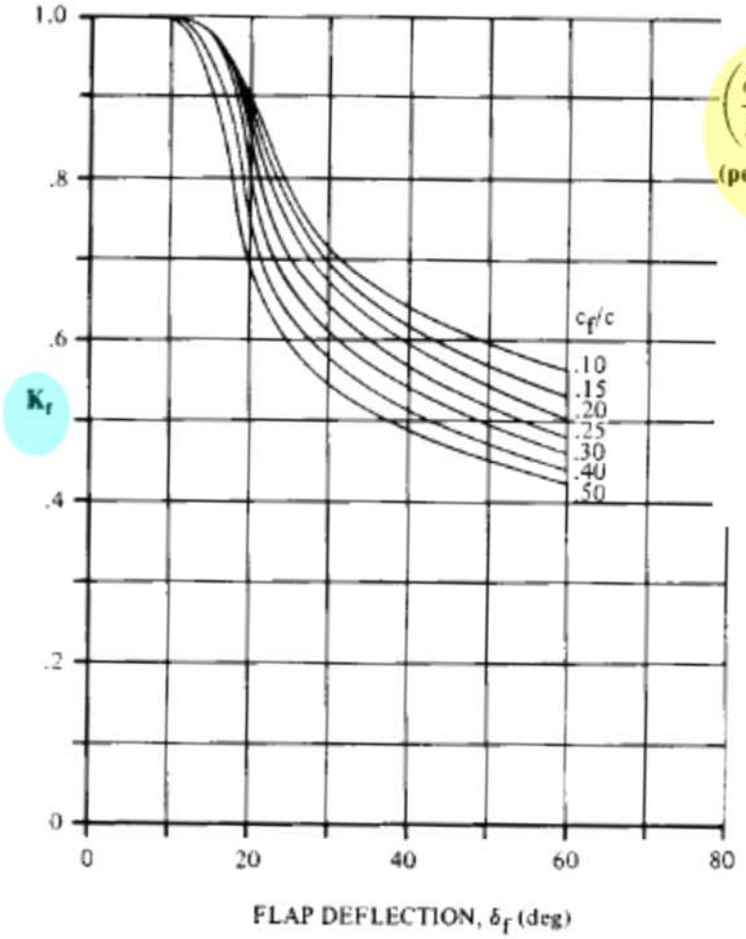

$\left(\frac{\partial C_\ell}{\partial \delta_f}\right)$ (per rad)

Fig. 16.7 Empirical correction for plain lift increment. (Ref. 37)

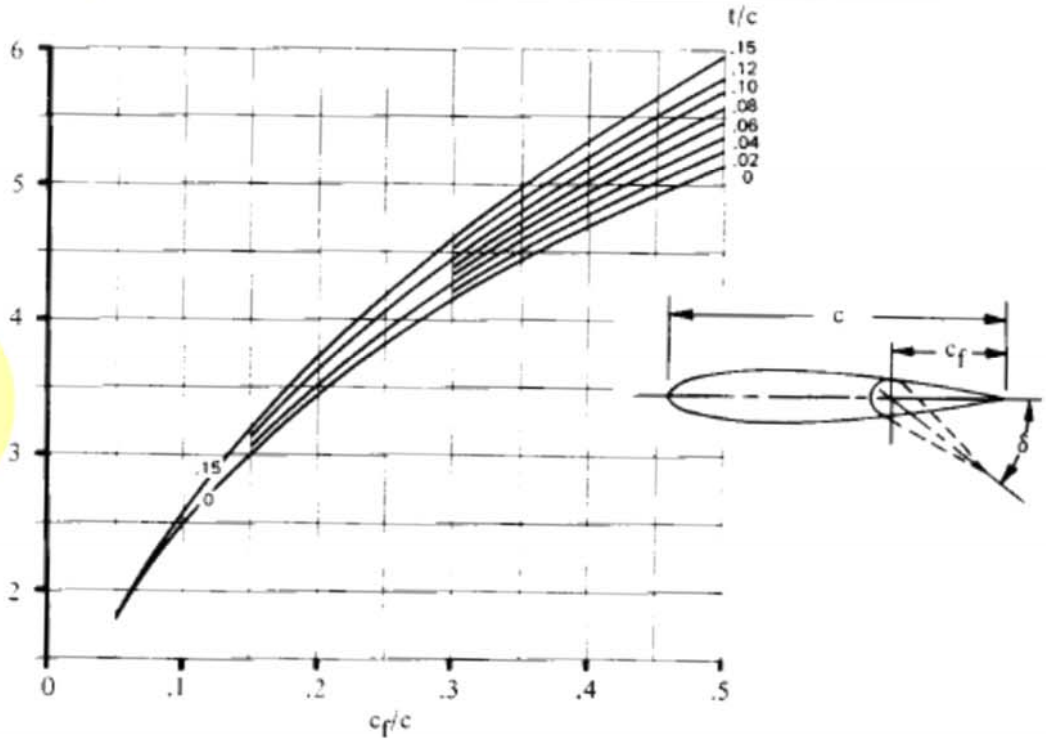

Fig. 16.6 Theoretical lift increment for plain flaps. (Ref. 37)

$$\Delta\alpha_{0L} = -\frac{1}{C_{L_\alpha}}\frac{\partial C_L}{\partial \delta_f}\delta_f$$

$$\frac{\partial C_L}{\partial \delta_f} = 0.9 K_f \left(\frac{\partial C_\ell}{\partial \delta_f}\right)' \frac{S_{\text{flapped}}}{S_{\text{ref}}} \cos\Lambda_{\text{H.L.}}$$

ángulo de la línea de bisagra

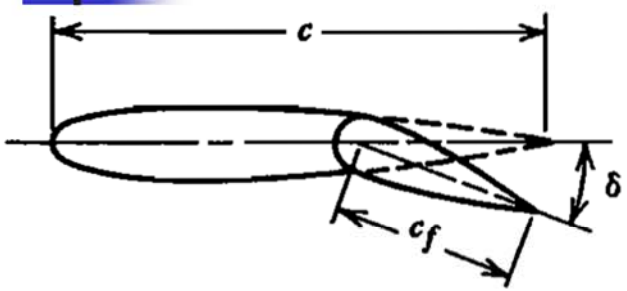

$$\frac{\partial C_L}{\partial \delta_f} = 0.9 K_f \left(\frac{\partial C_l}{\partial \delta_f}\right)' \frac{S_{\text{flapped}}}{S_{\text{ref}}} \cos\Lambda_{\text{H.L.}}$$

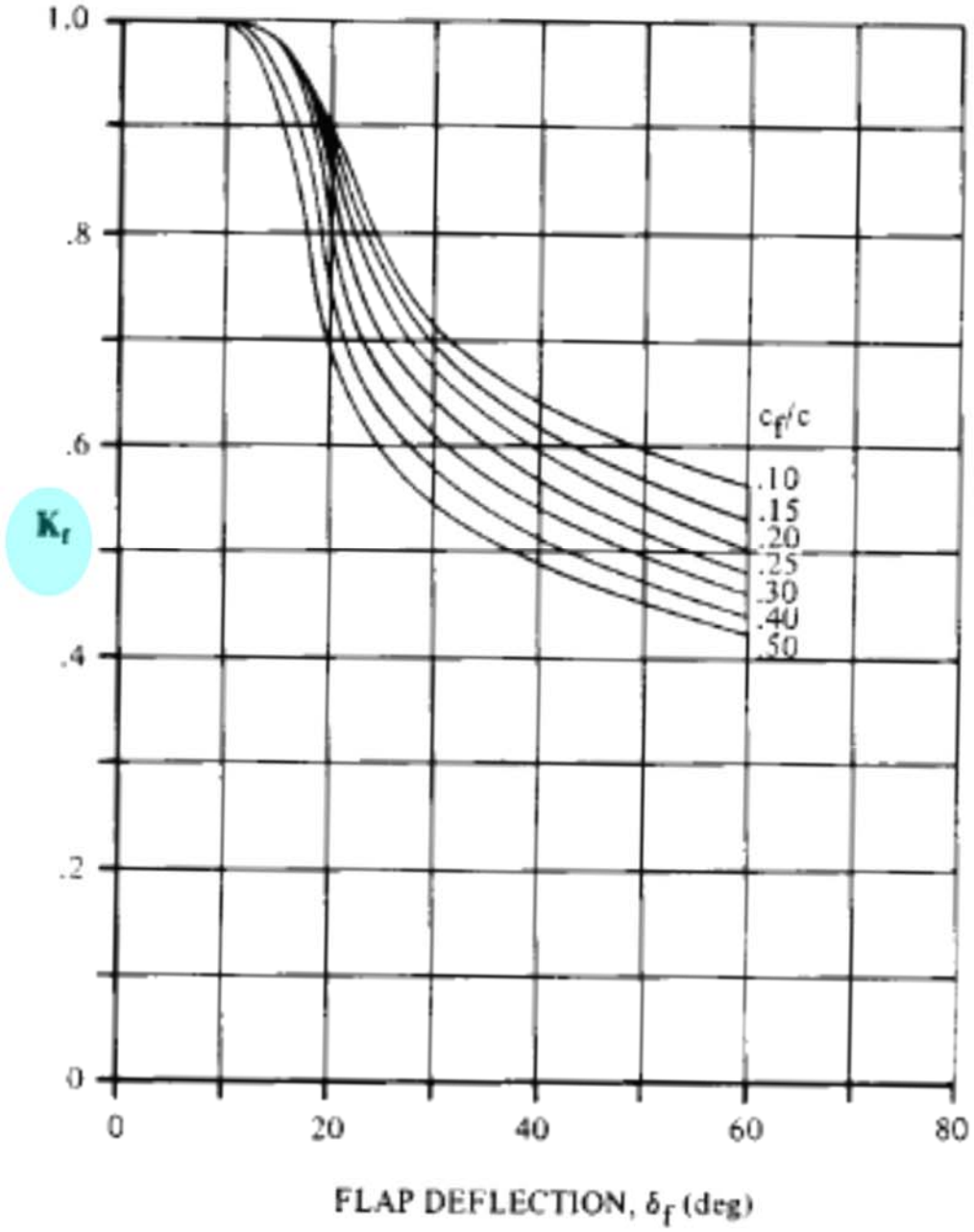

Fig. 16.7 Empirical correction for plain lift increment. (Ref. 37)

$$\frac{\partial C_L}{\partial \delta_f} = 0.9 K_f \left(\frac{\partial C_\ell}{\partial \delta_f} \right)' \frac{S_{\text{flapped}}}{S_{\text{ref}}} \cos\Lambda_{\text{H.L.}}$$

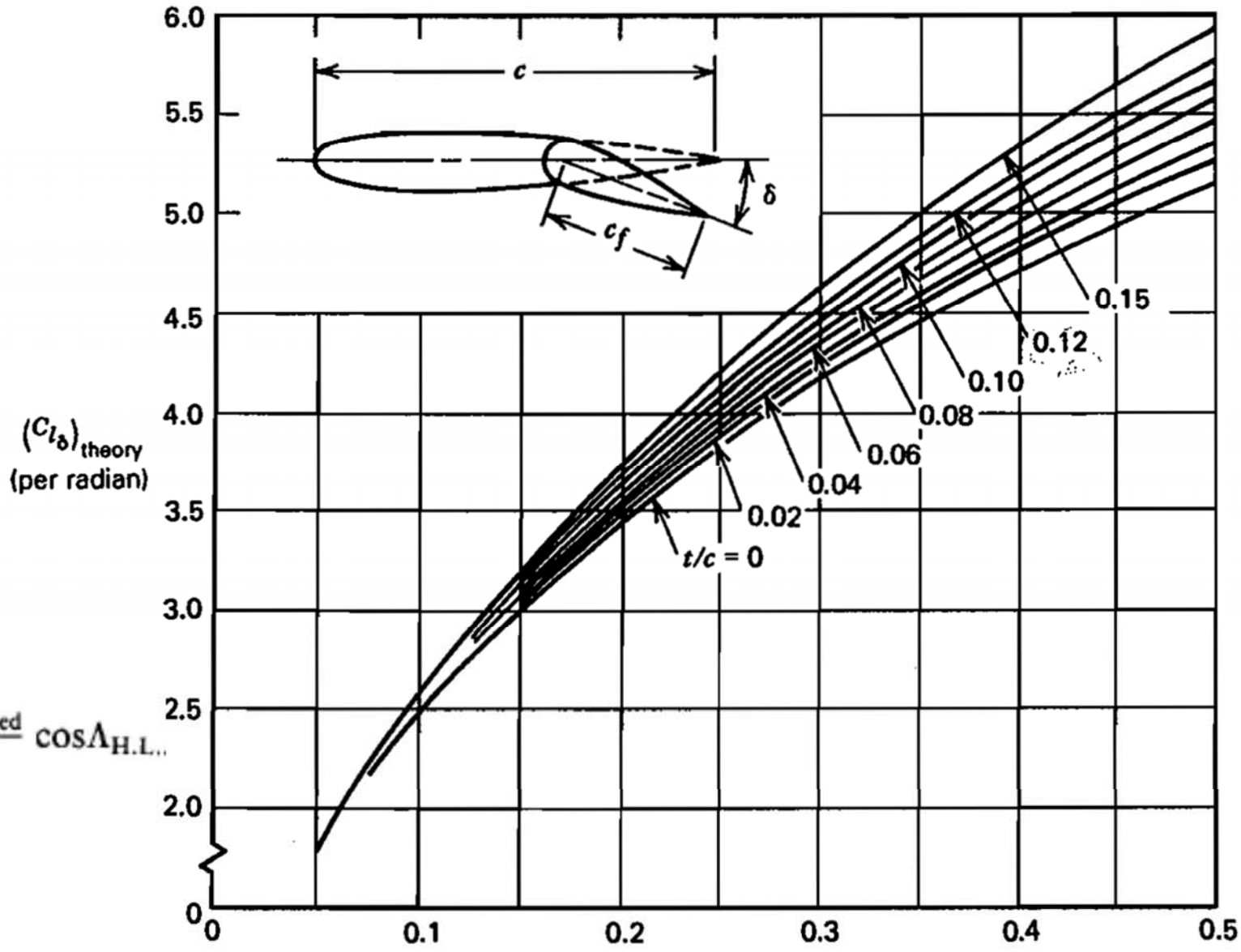

Control Derivatives

$C_{L_{\delta_e}}$

Método IV – (más preciso)

$C_{L_{\delta_e}} = C_{L_{h_\alpha}} \alpha_{\delta_e}$ $C_{L_{h_\alpha}} \rightarrow$ pendiente sustentación horizontal

The change in airplane angle-of-attack due to elevator deflection at zero deflection

$$\alpha_{\delta_e} = K_b \frac{c_{l_\delta}}{(c_{l_\delta})_{theory}} (c_{l_\delta})_{theory} \frac{k'}{c_{l_{\alpha_h}@M=0}} \frac{(\alpha_\delta)_{C_L}}{(\alpha_\delta)_{c_l}}$$

Método valido para determinar
- Canard
- Horizontal
- V-tail (proyección horizontal)

where:

K_b	is the elevator span factor.
c_{l_δ}	is the derivative of airfoil lift coefficient with flap deflection.
$(c_{l_\delta})_{theory}$	is the theoretical derivative of airfoil lift coefficient with flap deflection.
k'	is the correction factor for nonlinearities at high elevator deflection angles.
$c_{l_{\alpha_h}@M=0}$	is the horizontal tail airfoil lift curve slope at horizontal tail mean geometric chord at M=0 and Re=9x10^6.
$\frac{(\alpha_\delta)_{C_L}}{(\alpha_\delta)_{c_l}}$	is the three dimensional flap effectiveness ratio.

Control Derivatives - I

$C_{L_{\delta_e}}$

The change in airplane angle-of-attack due to elevator deflection at zero deflection

$$\alpha_{\delta_e} = K_b \frac{c_{l_\delta}}{(c_{l_\delta})_{theory}} \frac{(c_{l_\delta})_{theory}}{c_{l_{\alpha_h}\,@\,M=0}} \frac{k'}{} \frac{(\alpha_\delta)_{C_L}}{(\alpha_\delta)_{c_l}}$$

$$\frac{c_{l_\delta}}{(c_{l_\delta})_{theory}} = f\left(\frac{c_e}{c_h}, \frac{c_{l_{\alpha_h}\,@\,M=0}}{(c_{l_{\alpha_h}})_{theory}}\right) \quad \Rightarrow \text{Fig A3}$$

$$(c_{l_{\alpha_h}})_{theory} = 2\pi + 5.0525\left(\frac{t}{c}\right)_h \quad \Rightarrow \quad \left(\frac{t}{c}\right)_h = \frac{\left(\frac{t}{c}\right)_{r_h} - \frac{\eta_{o_e} + \eta_{i_e}}{2}\left[\left(\frac{t}{c}\right)_{r_h} - \left(\frac{t}{c}\right)_{t_h}\lambda_h\right]}{1 - \frac{\eta_{o_e} + \eta_{i_e}}{2}(1-\lambda_h)}$$

Fig A4

$$(c_{l_\delta})_{theory} = f\left(\frac{c_e}{c_h}, \left(\frac{t}{c}\right)_h\right)$$

Fig A5

$$k' = f\left(\frac{c_e}{c_h}, \delta_e\right)$$

Fig A6

$$\frac{(\alpha_\delta)_{C_L}}{(\alpha_\delta)_{c_l}} = f\left(AR_h, \frac{c_e}{c_h}\right)$$

Control Derivatives - II

$C_{L_{\delta_e}}$

The change in airplane angle-of-attack due to elevator deflection at zero deflection

$$K_b = K_{b_o} - K_{b_i}$$

K_{b_o} - is the outboard elevator span factor.
K_{b_i} - is the inboard elevator span factor.

function of the elevator inboard and outboard stations, and the horizontal tail taper ratio

1) Determinar η_i y η_0 - define la envergadura de la superficie de control (Fig A1)
2) Determinar $\Delta\eta_i = \eta_0 - \eta_i$ (Fig A1) y utilizarlo para determinar $K_2 = K_b$ (Fig A2)

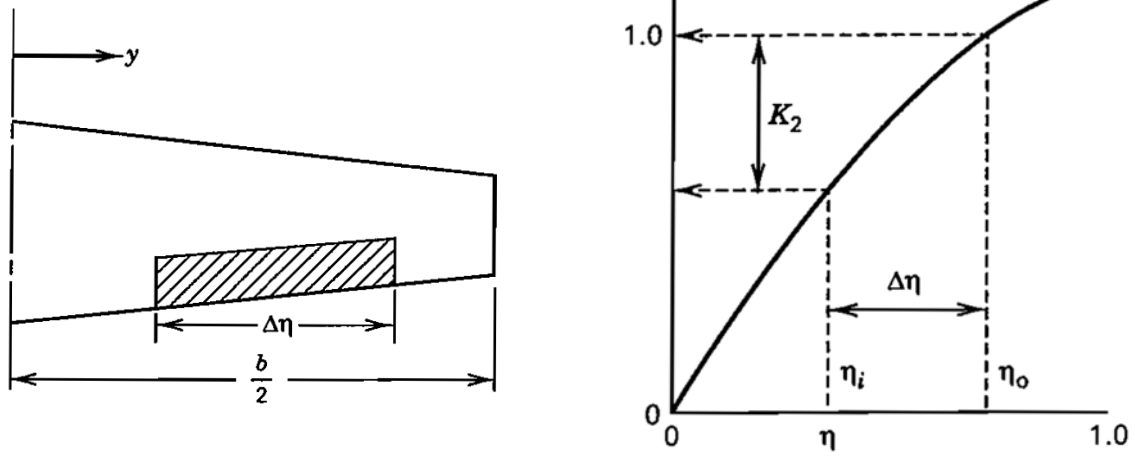

Fig A1

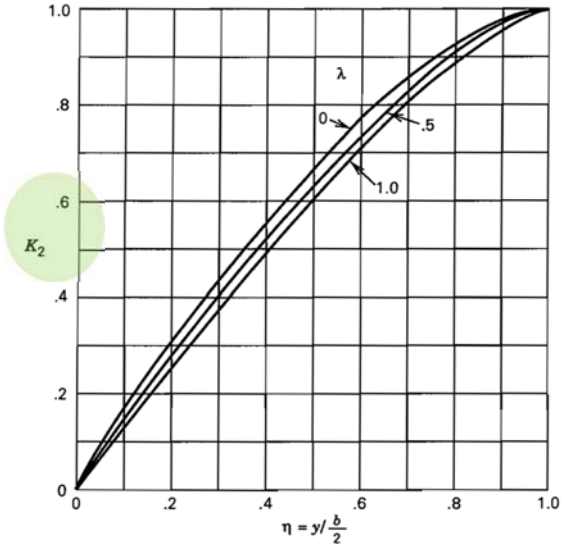

Figure B.2,3 Span factor for inboard flaps.

Fig A2

Fig A31I

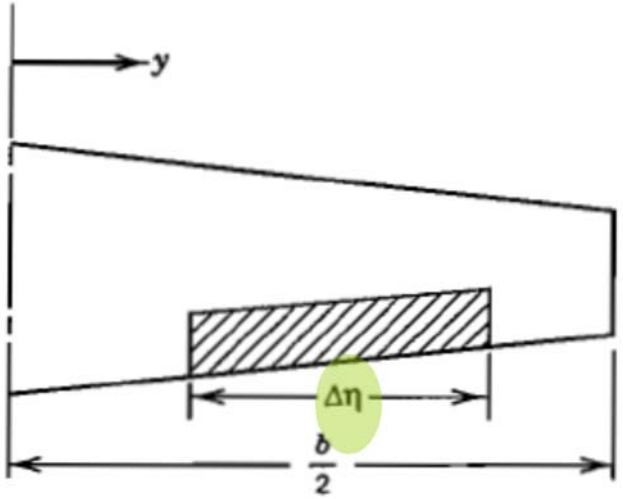

$K_b = K_2$

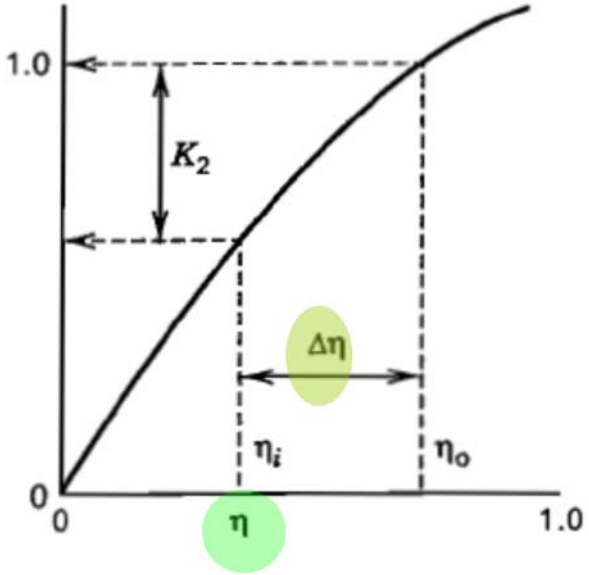

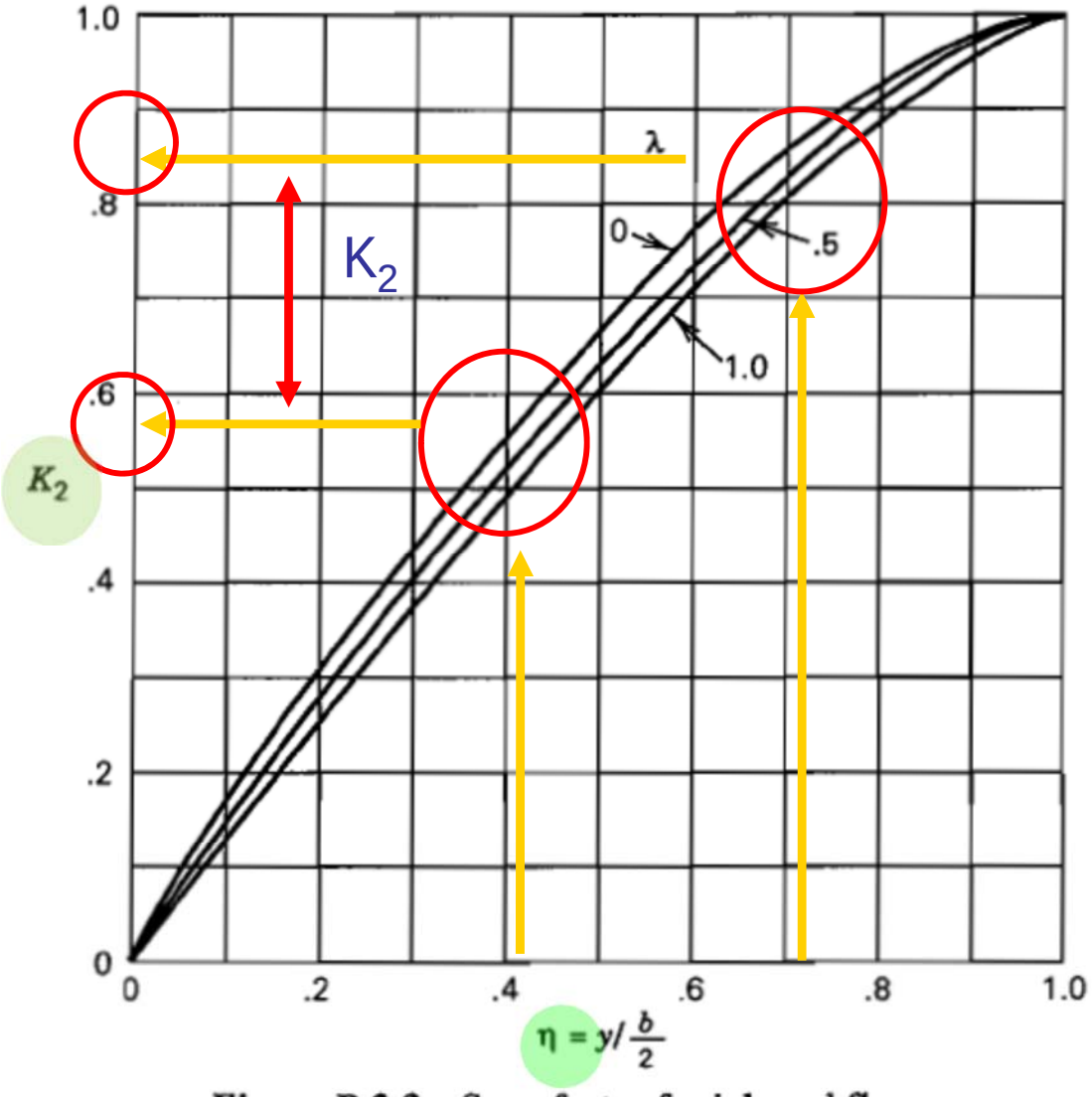

Figure B.2,3 Span factor for inboard flaps.

Fig A1

where:

η_{i_e}	is the elevator inboard station in terms of the horizontal tail half span.
η_{o_e}	is the elevator outboard station in terms of the horizontal tail half span.
λ_h	is the horizontal tail taper ratio.

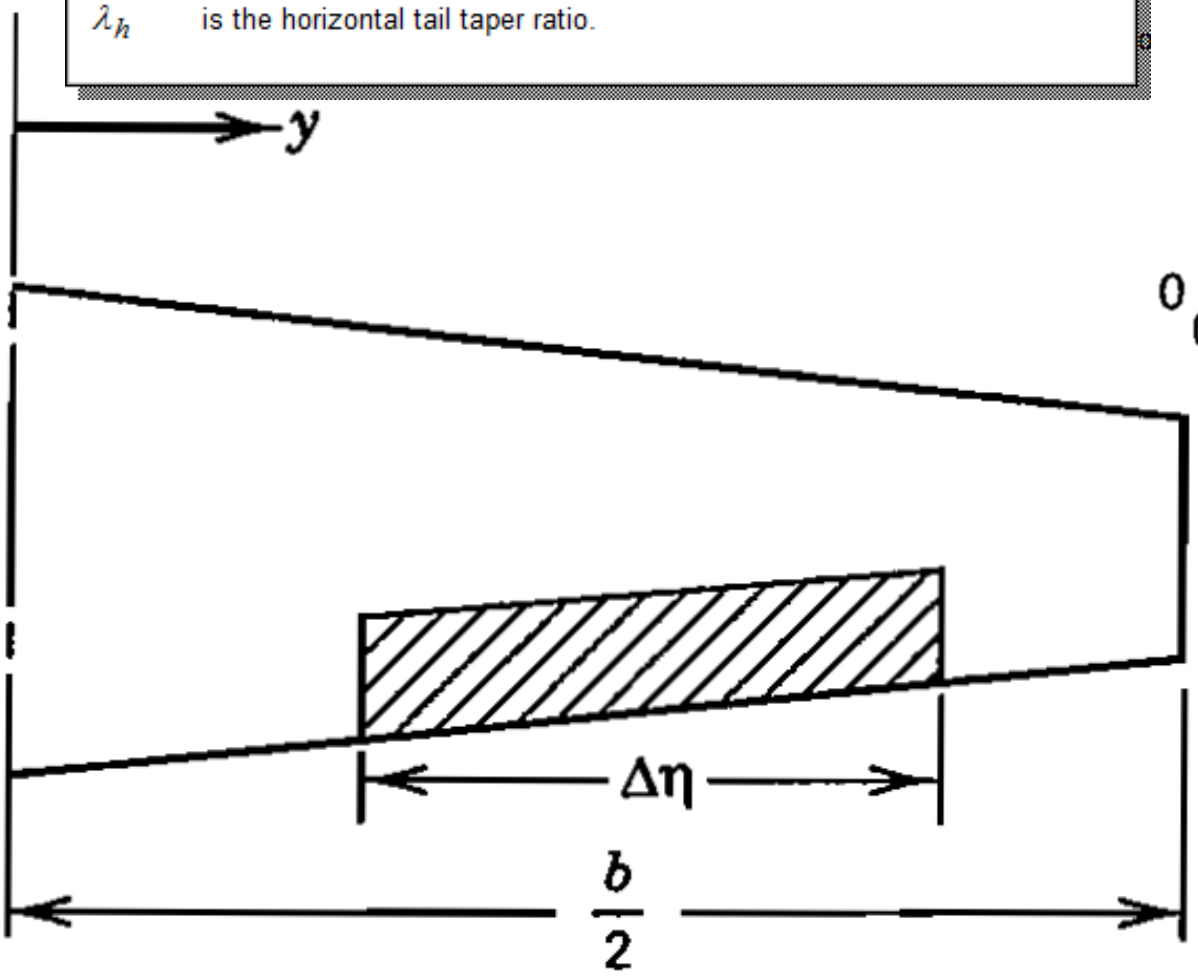

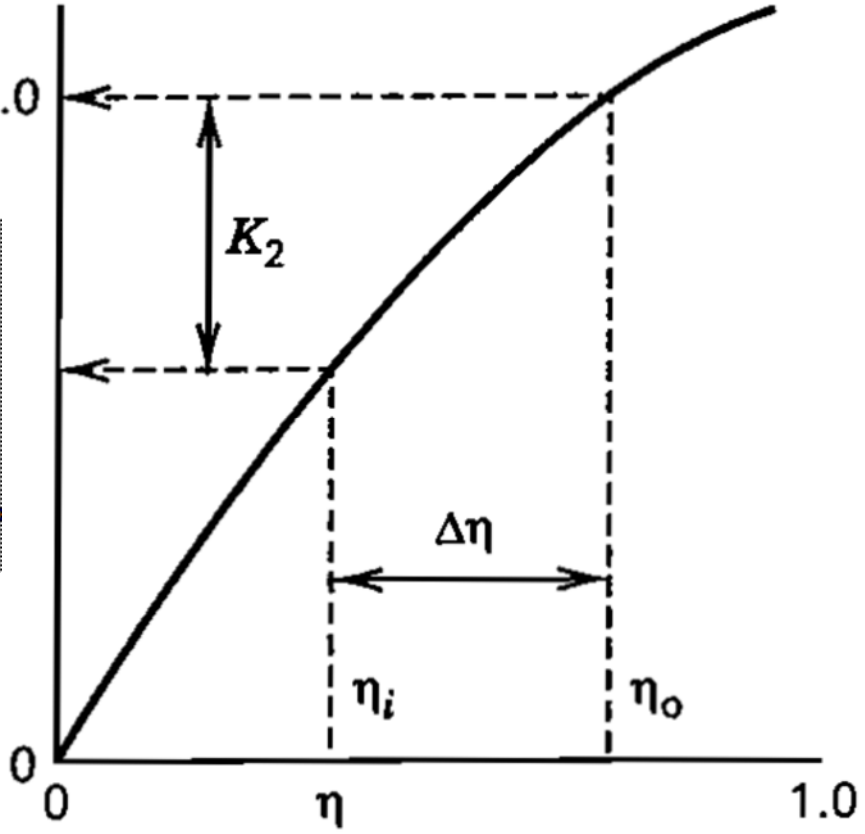

Elevator span factor

Fig A2

Elevator span factor

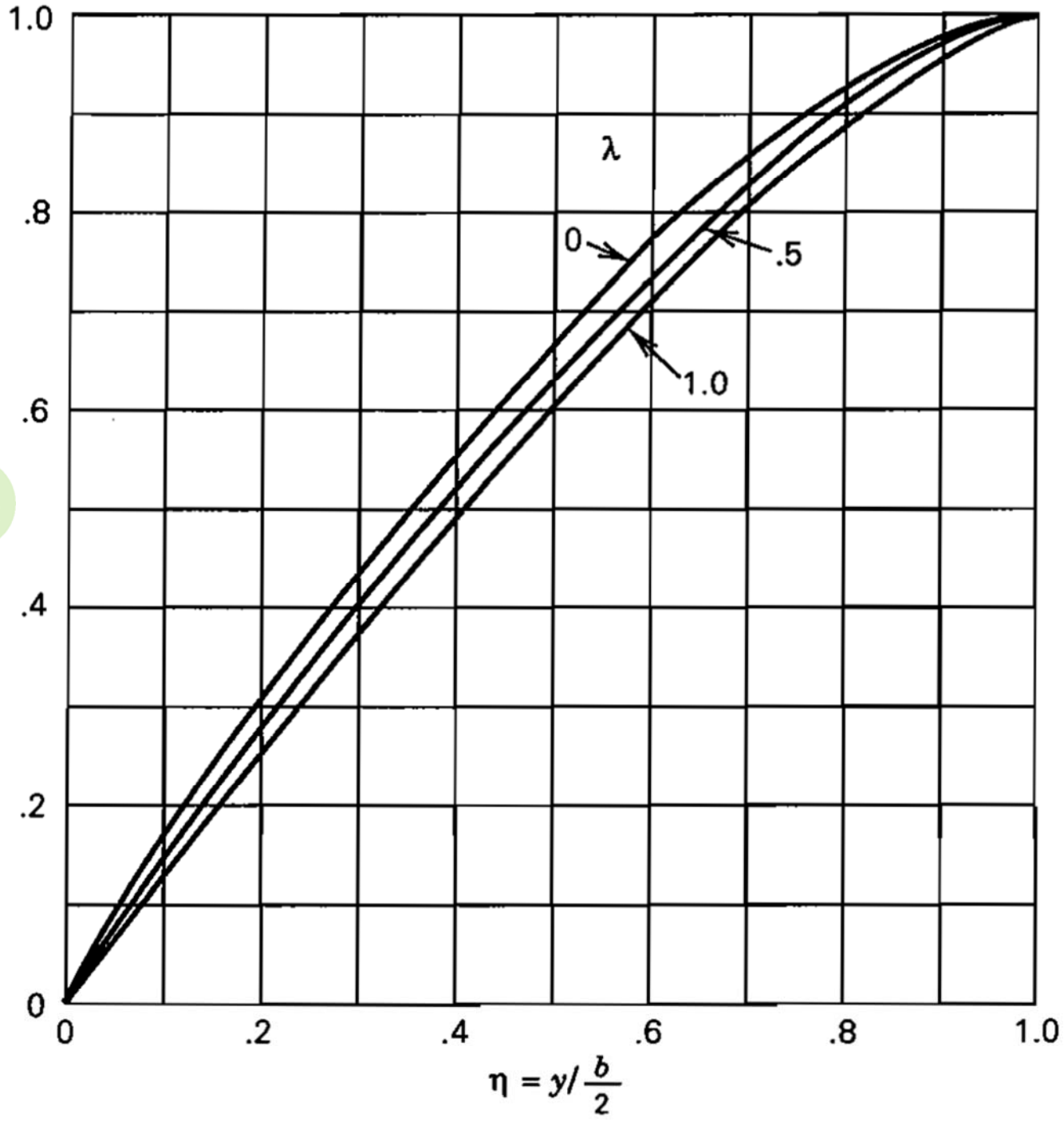

Figure B.2,3 **Span factor for inboard flaps.**

Fig A3

$C_{L_{\delta_e}}$

The correction factor for flap lift is obtained from Figure 8.15 in *Airplane Design Part VI* and is a function of the elevator chord to horizontal tail chord ratio and the sectional lift curve slope to theoretical lift curve slope ratio:

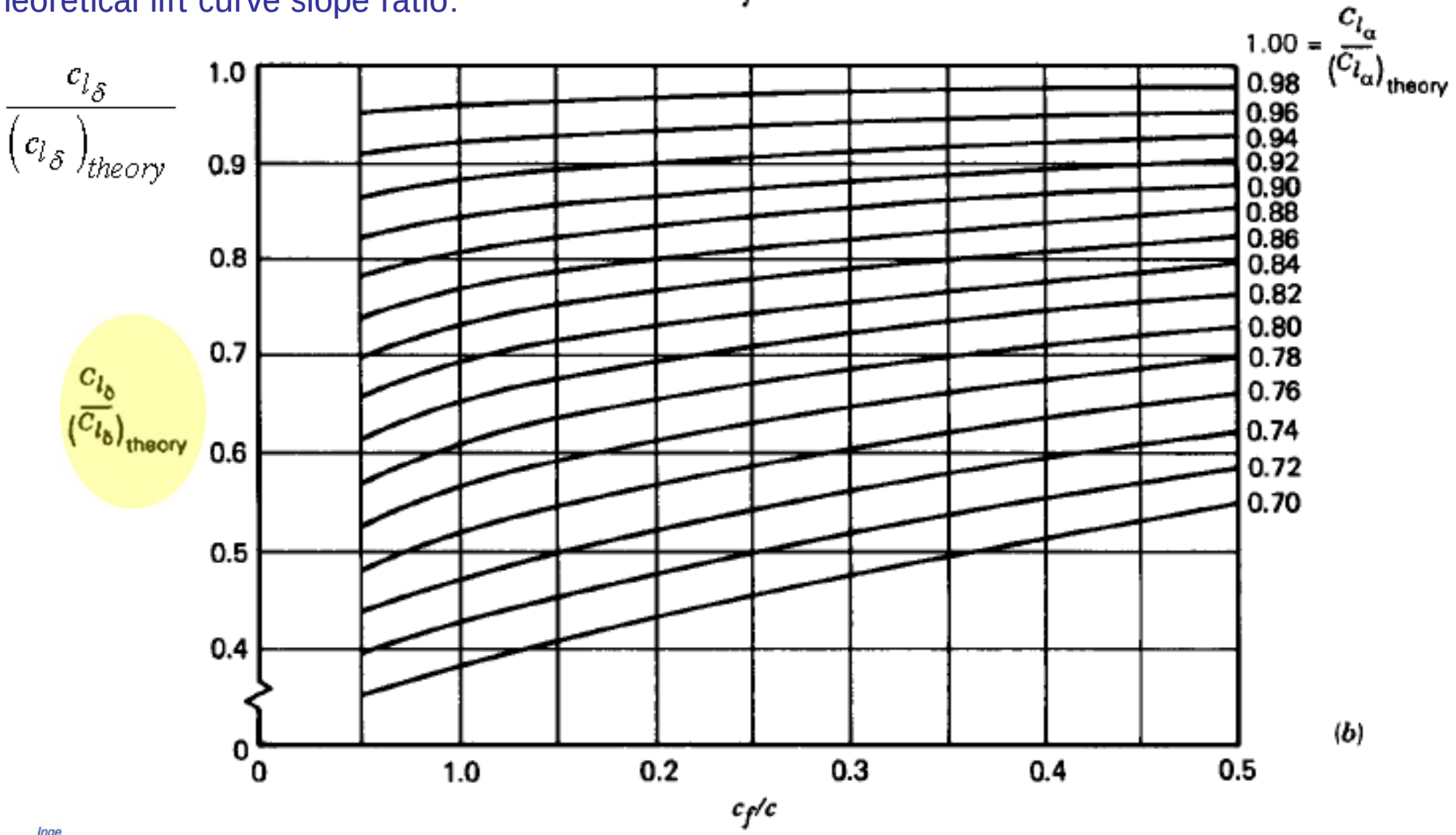

Fig A4

$C_{L_{\delta_e}}$

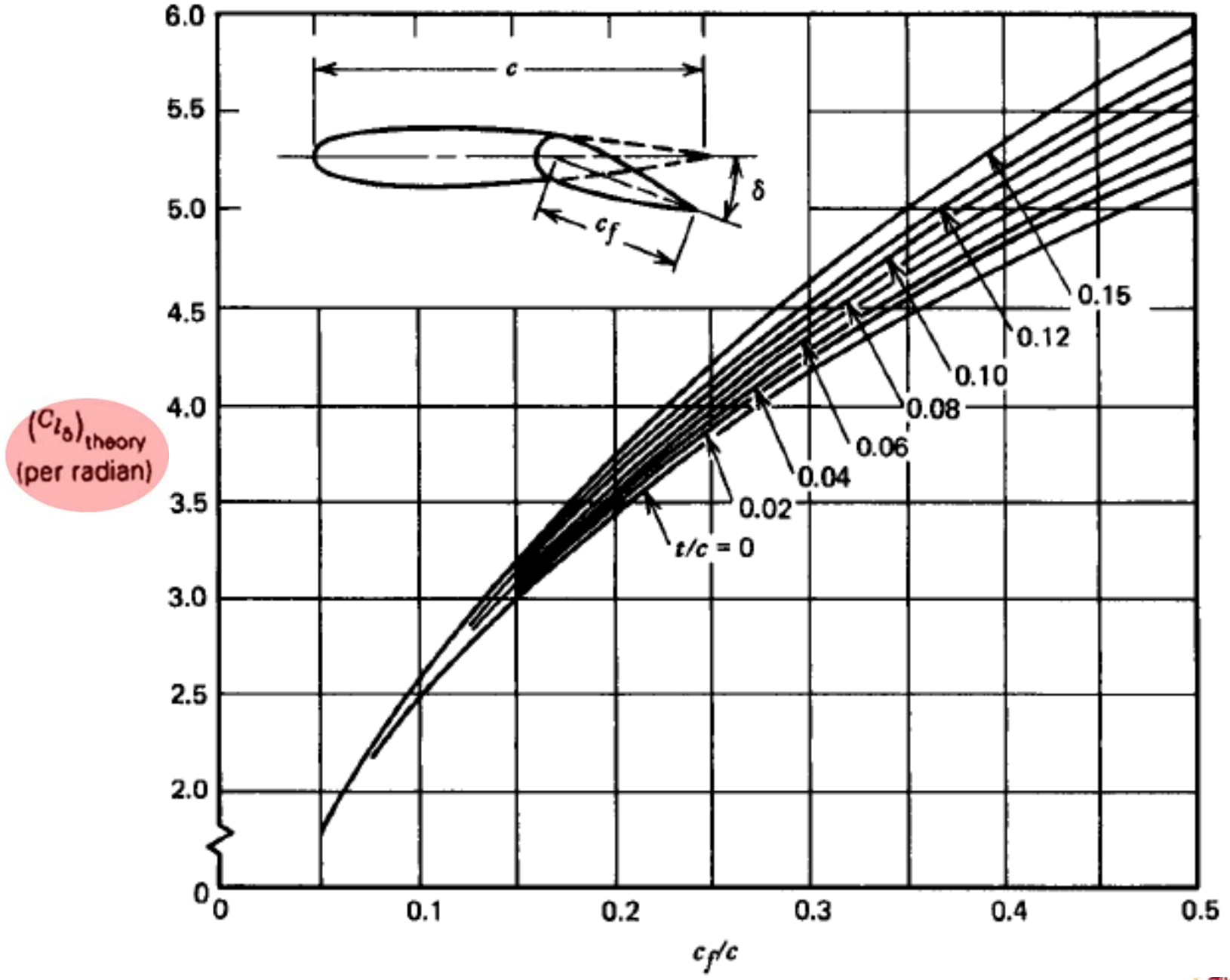

Fig A5

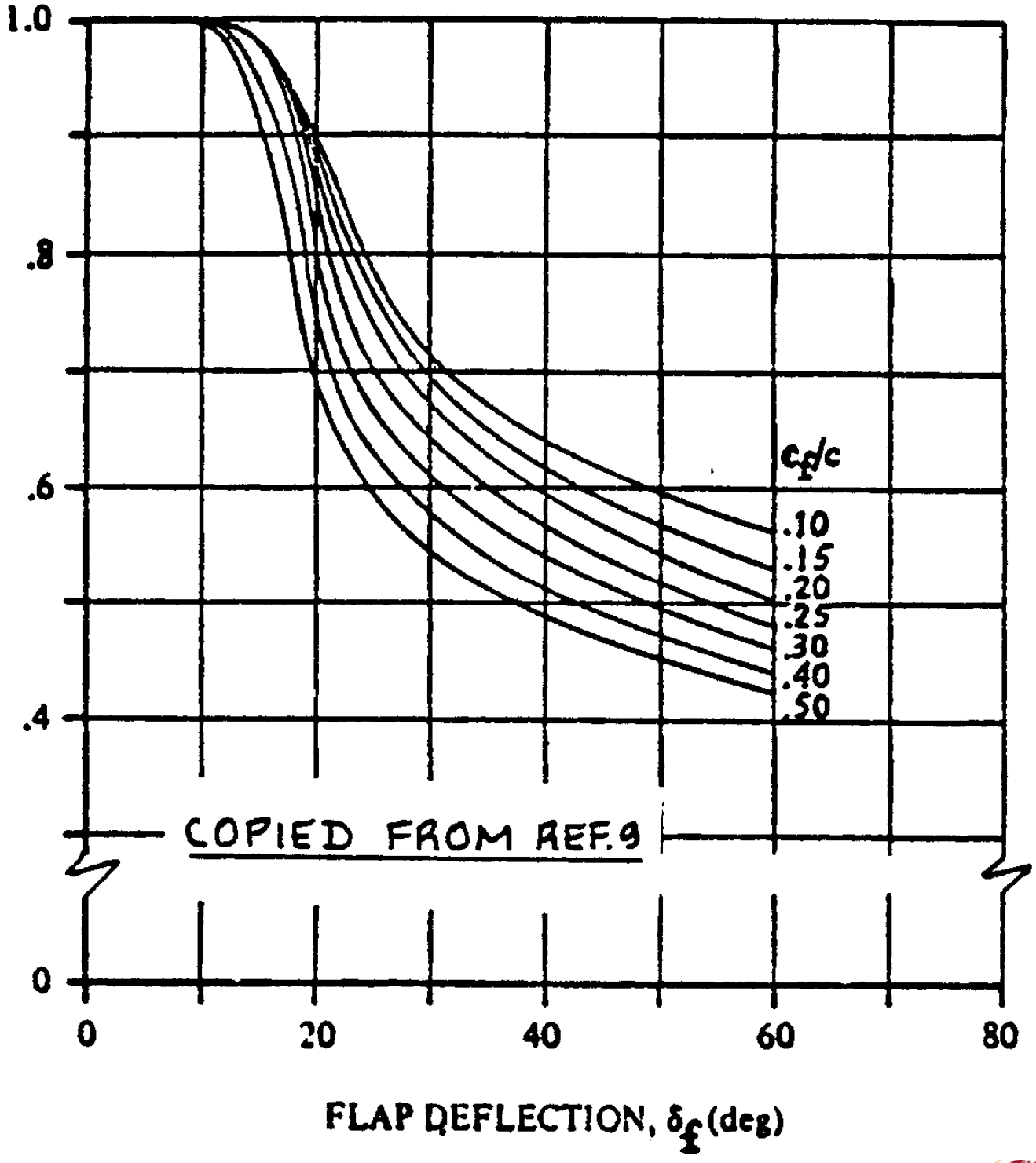
1.0
.8
.6
.4
0
0
20
40
60
80
c_f/c
.10
.15
.20
.25
.30
.40
.50
COPIED FROM REF.9
FLAP DEFLECTION, δ_f (deg)

Fig A6

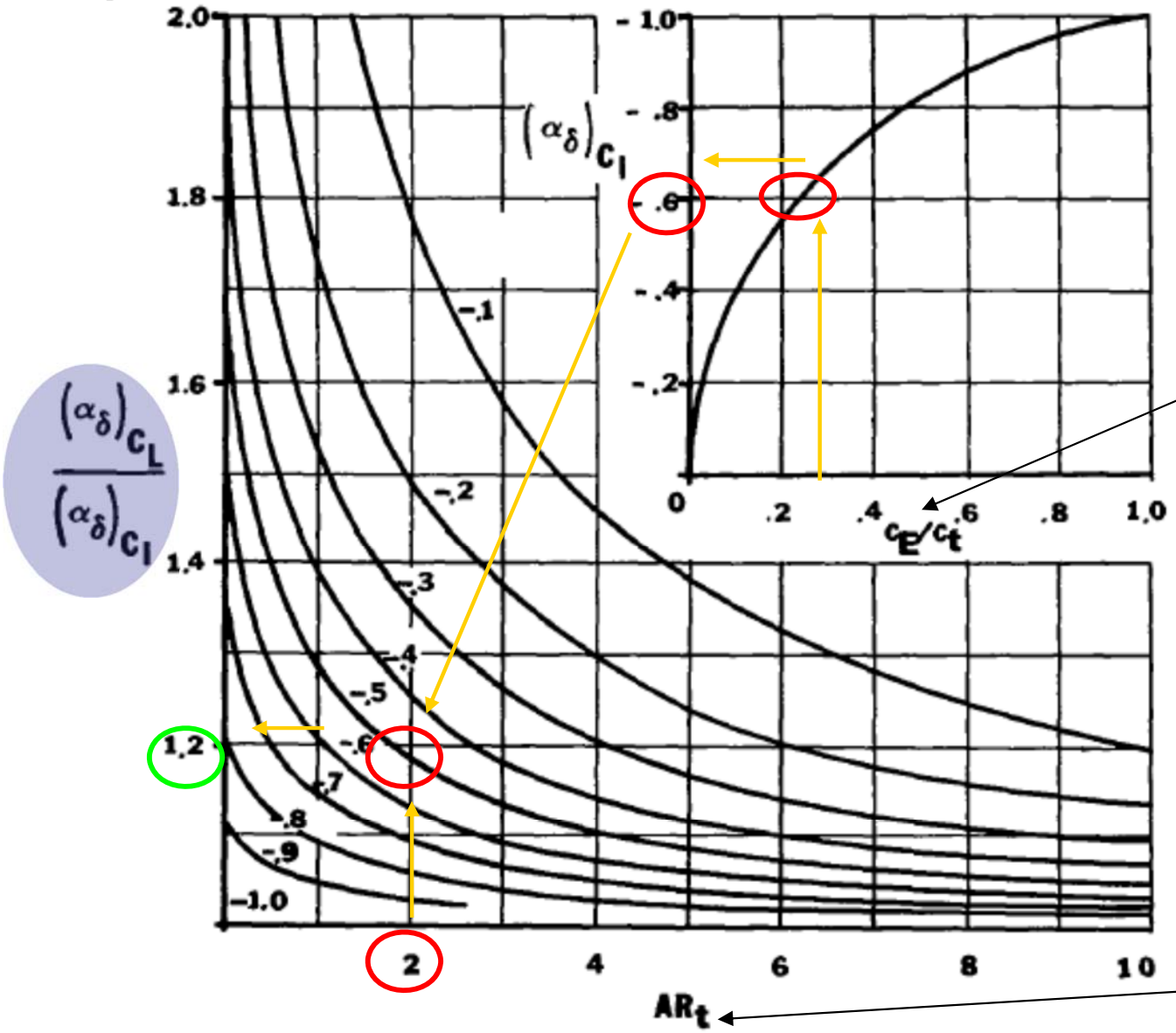

Figure 16. Flap chord factor.

Relación entre cuerdas superficie de control/ estabilizador

- Selección c_E/c_t
- Genera $(\alpha_\delta)_{Cl}$
- Selección AR_t y $(\alpha_\delta)_{Cl}$
-Genera $(\alpha_\delta)_{CL}$ $(\alpha_\delta)_{Cl}$

Alargamiento del estabilizador

Fig A6

$$\frac{(\alpha_\delta)_{C_L}}{(\alpha_\delta)_{c_l}}$$

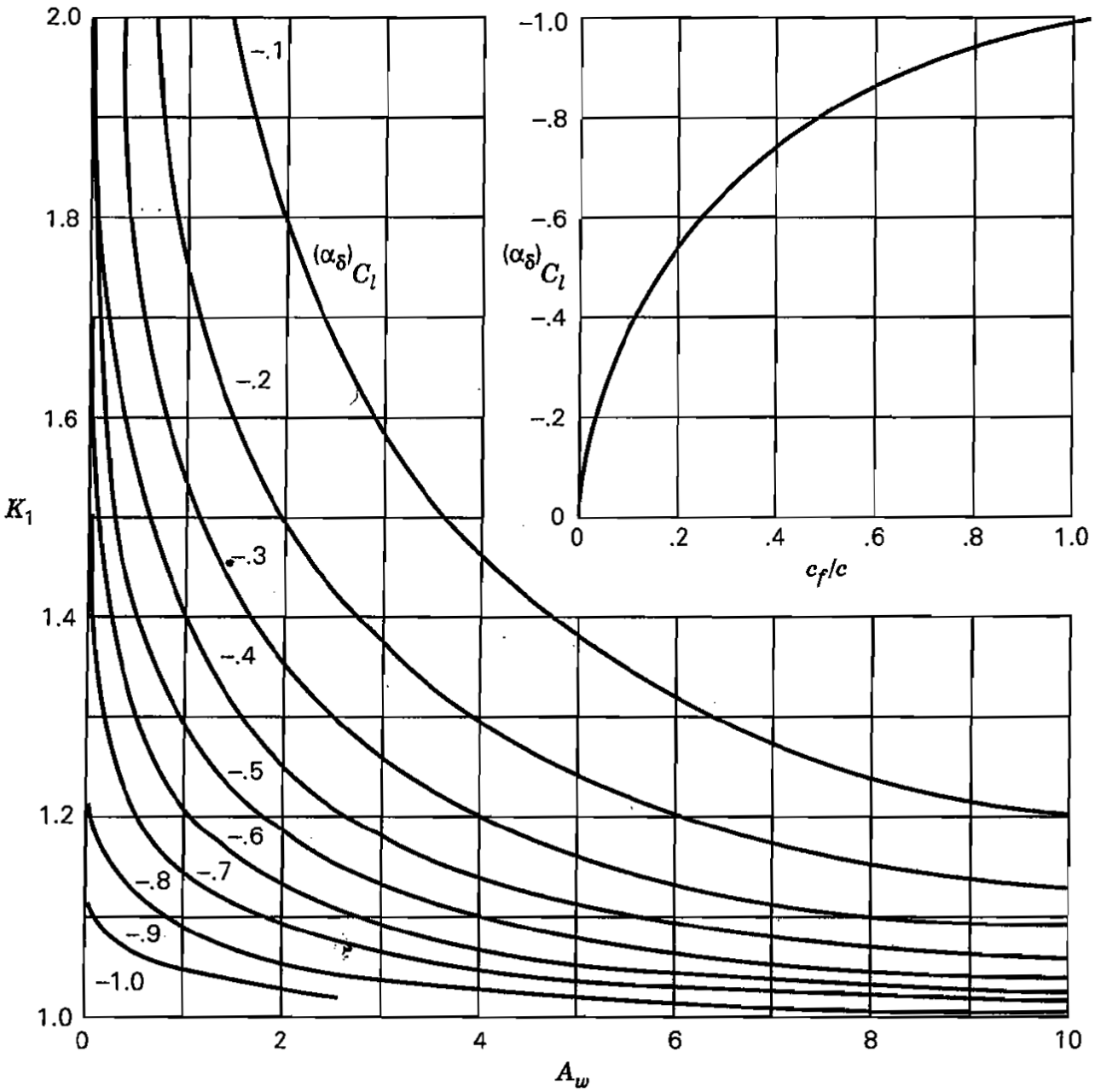

Figure B.2,2 Flap-chord factor.

Control Derivatives $C_{D_{\delta_e}}$

$$C_{D_{\delta_e}} = \alpha_{\delta_e} C_{D_{i_h}}$$

$$C_{D_{i_h}} = 2\frac{C_{L_o}}{\pi AR_w e}\eta_{h_{p.off}}\left(\frac{S_h}{S_w}\right)C_{L_{h_\alpha}}$$

where:

C_{L_o}	is the airplane zero-angle-of-attack lift coefficient including flap effects.
AR_w	is the wing aspect ratio.
e	is the Oswald efficiency factor.
$C_{L_{h_\alpha}}$	is the horizontal tail lift curve slope.
$\eta_{h_{p.off}}$	is the horizontal tail dynamic pressure ratio without power effects.
S_h	is the horizontal tail area.
S_w	is the wing area.

Método valido para determinar
- Canard
- Horizontal
- V-tail (proyección horizontal)

Se puede asumir como despreciable en 1ª estimación

Control Derivatives $C_{M_{\delta_e}}$

Is the change in pitching moment coefficient with changes in elevator deflection

$$C_{M_{\delta_e}} = -\frac{l_t}{c} C_{L_{\delta_e}}$$

Método valido para determinar
- Canard
- Horizontal
- V-tail (proyección horizontal)

Modificar brazo l_t ⇒

$$l_c = x_{ac_c} - x_{cg}$$
$$l_t = x_{ac_t} - x_{cg}$$
$$l_{vee} = x_{ac_{vee}} - x_{cg}$$

Control Derivatives

$C_{Y_{\delta_a}}$

is the change in sideforce coefficient with variation in aileron deflection

$$C_{Y_{\delta_a}} \approx 0$$

Control Derivatives

$C_{L_{\delta a}}$

ailero effectiveness or " aileron power", is the variation in rolling moment coefficient with change in aileron deflection

$$C_{\ell_{\delta_A}} = \frac{2(C_{L_\alpha})_w \tau}{S_w b_w} \int_a^b c\, y\, dy.$$

c, as a function of the spanwise distance, $c = c_R \left[1 - \frac{y}{b_w/2}(1-\lambda)\right]$, c_R = root chord.

Alternative method to integration

$$C_{\ell_{\delta_A}} = \frac{C_{l_{\delta_A}}}{\tau} \tau$$

Fig A29

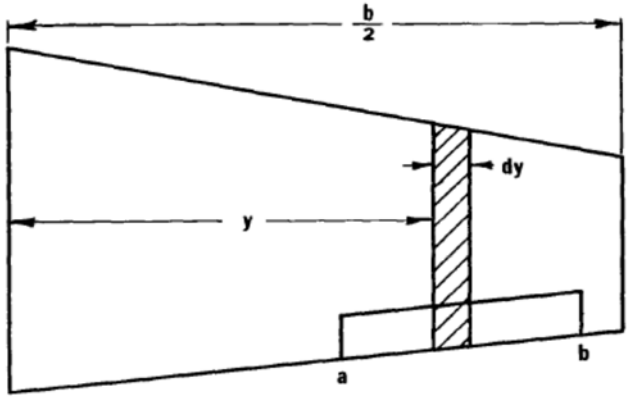

Figure 40. Illustration of strip integration.

Fig A30

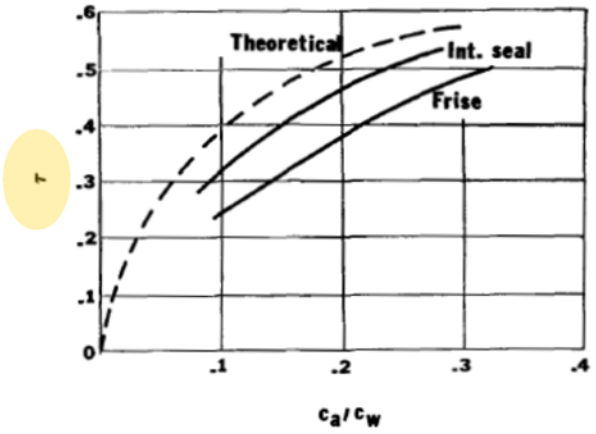

Figure 41. Values for τ as a function of aileron chord to wing chord ratio.

Fig A31

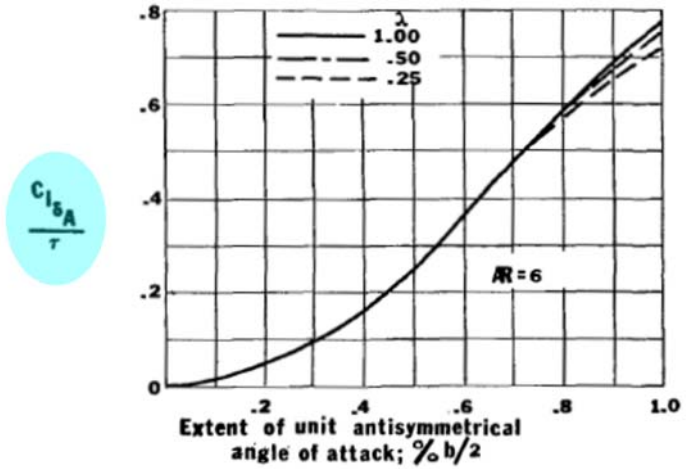

Figure 42. Values for $(C_{\ell_{\delta_A}}/\tau)$ as a function of the extent of unit antisymmetrical angle of attack.

Fig A29

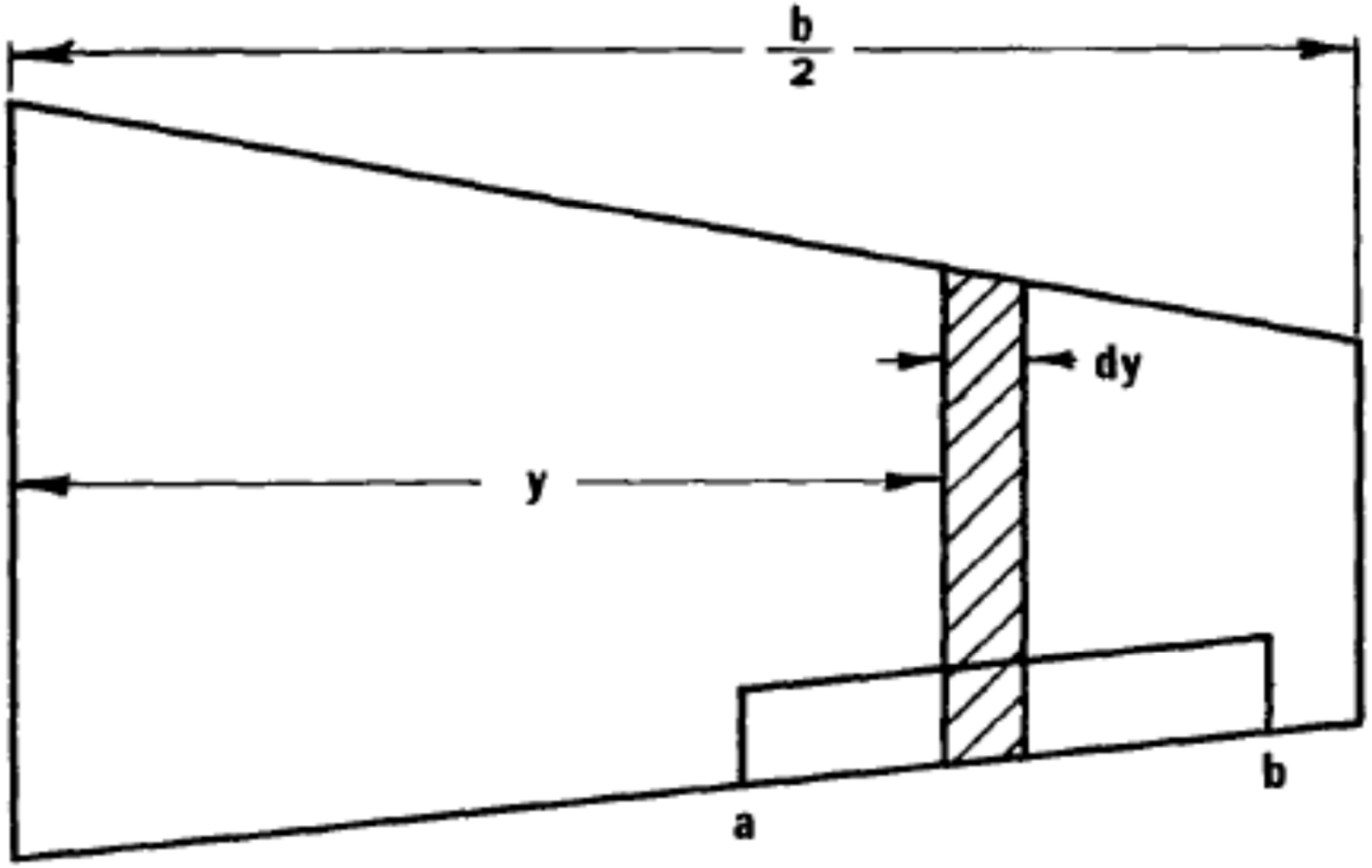

Figure 40. Illustration of strip integration.

Fig A30

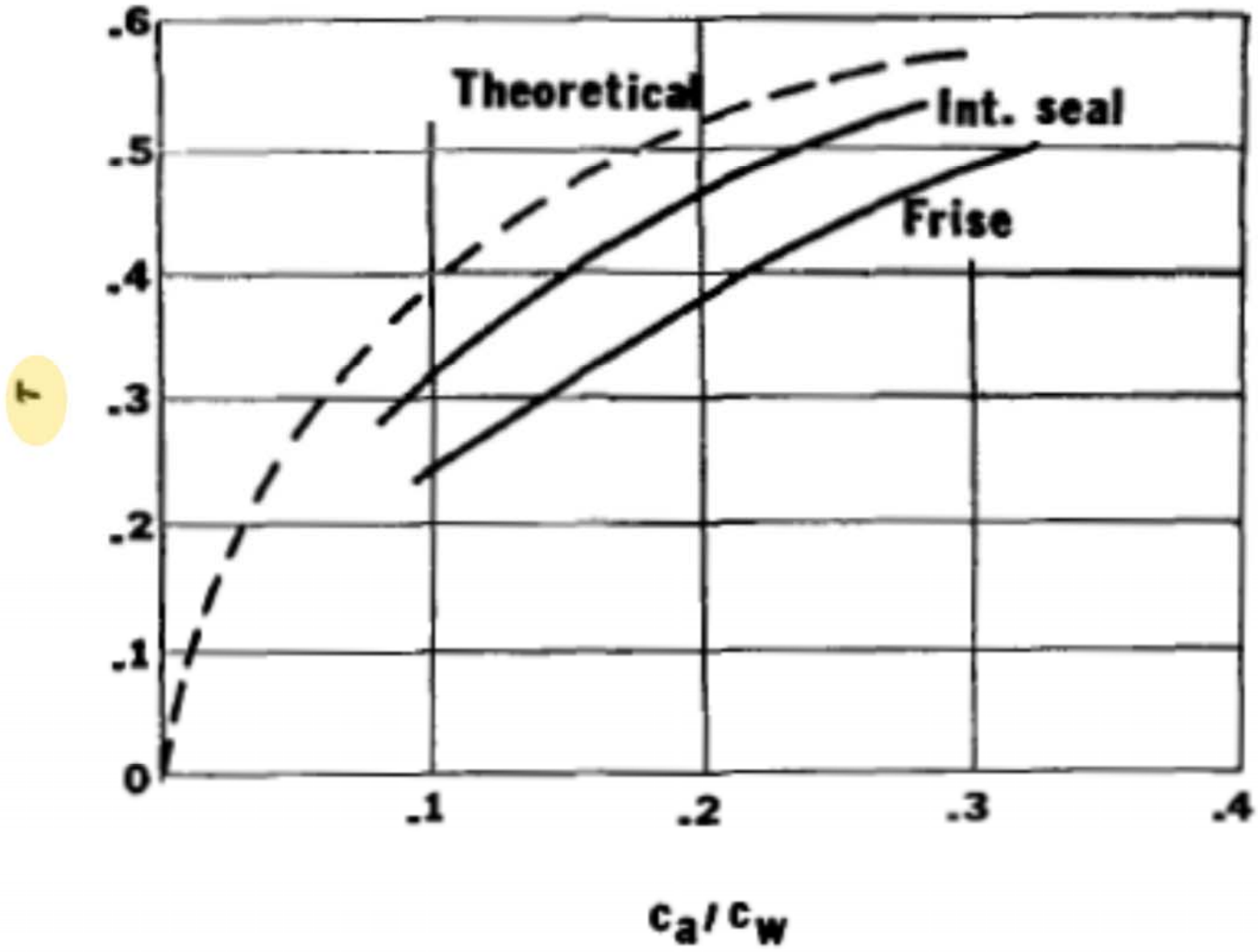

Figure 41. Values for τ as a function of aileron chord to wing chord ratio.

Fig A31

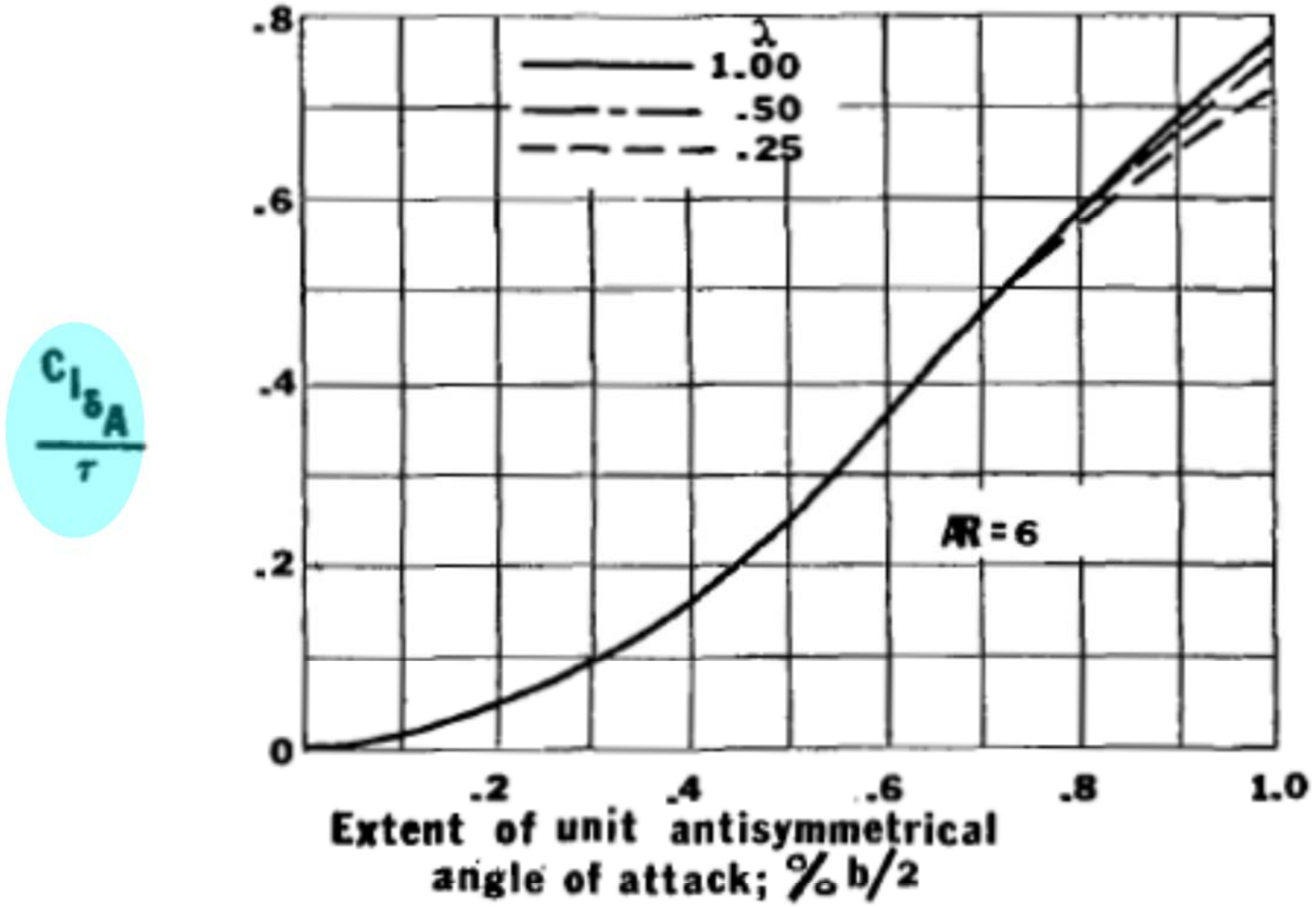

Figure 42. Values for ($C_{\ell_{\delta A}}/\tau$) as a function of the extent of unit antisymmetrical angle of attack.

Contribución de los alerones

- Se utiliza un método de franjas. Se divide los alerones en franjas

Considera el efecto de los 2 alerones

$$C_{\ell_{\delta_a}} = \frac{2\Sigma K_f \left(\frac{\partial C_L}{\partial \delta_f}\right)' Y_i S_i \cos\Lambda_{H.L.}}{S_w b}$$

Brazo del momento de la franja

Si se emplea una sola franja se puede estimar la efectividad de la superficie de control (alerón) dCL/dδf en función del ratio de superficies Sflapped/Sref

$$\frac{\partial C_L}{\partial \delta_f} = 0.9 K_f \left(\frac{\partial C_\ell}{\partial \delta_f}\right)' \frac{S_{flapped}}{S_{ref}} \cos\Lambda_{H.L.}$$

Fig 31A

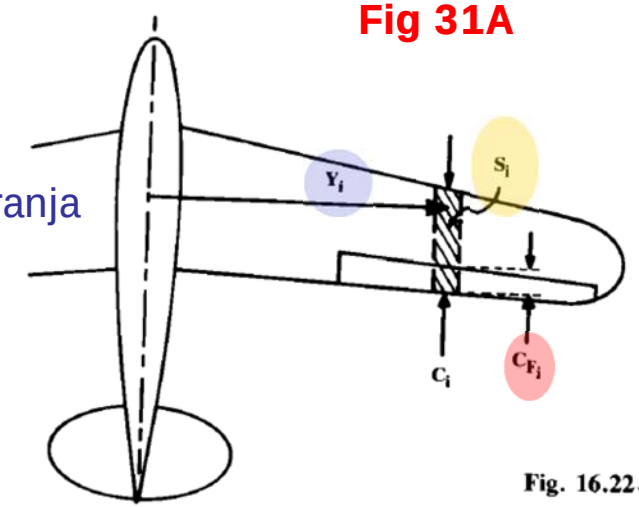

Fig. 16.22

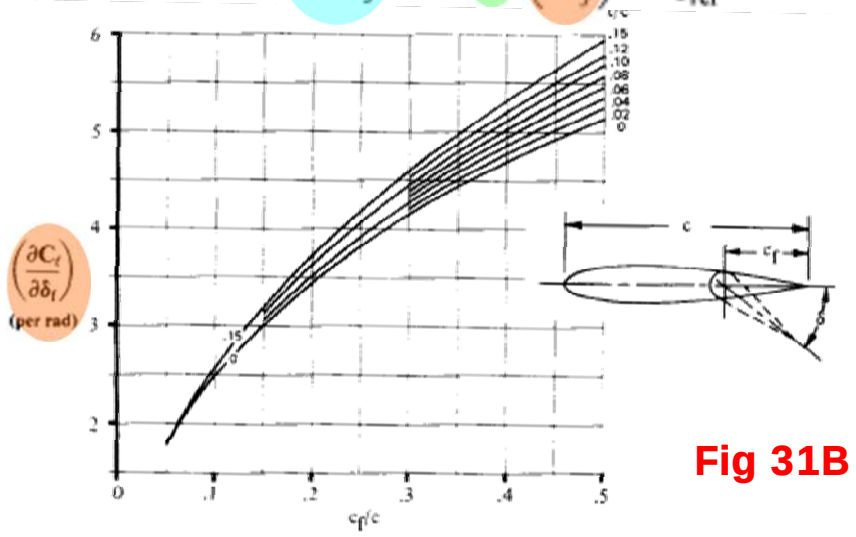

Fig 31B

Fig. 16.6 Theoretical lift increment for plain flaps. (Ref. 37)

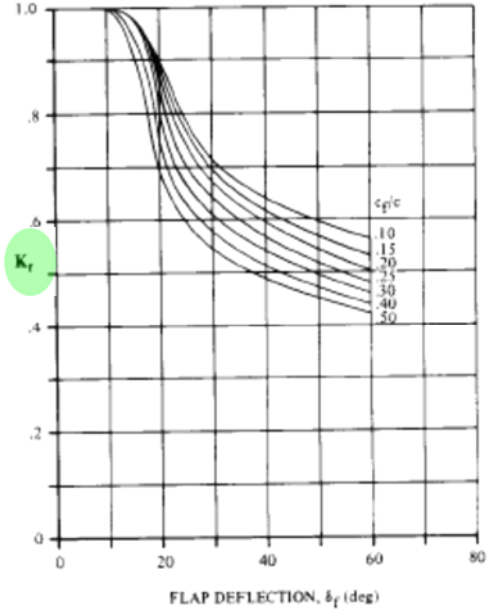

Fig 31C

Fig. 16.7 Empirical correction for plain lift increment. (Ref. 37)

Fig A31A

$$C_{\ell_{\delta_a}} = \frac{2\Sigma K_f \left(\frac{\partial C_L}{\partial \delta_f}\right)' Y_i S_i \cos\Lambda_{\text{H.L.}}}{S_w b}$$

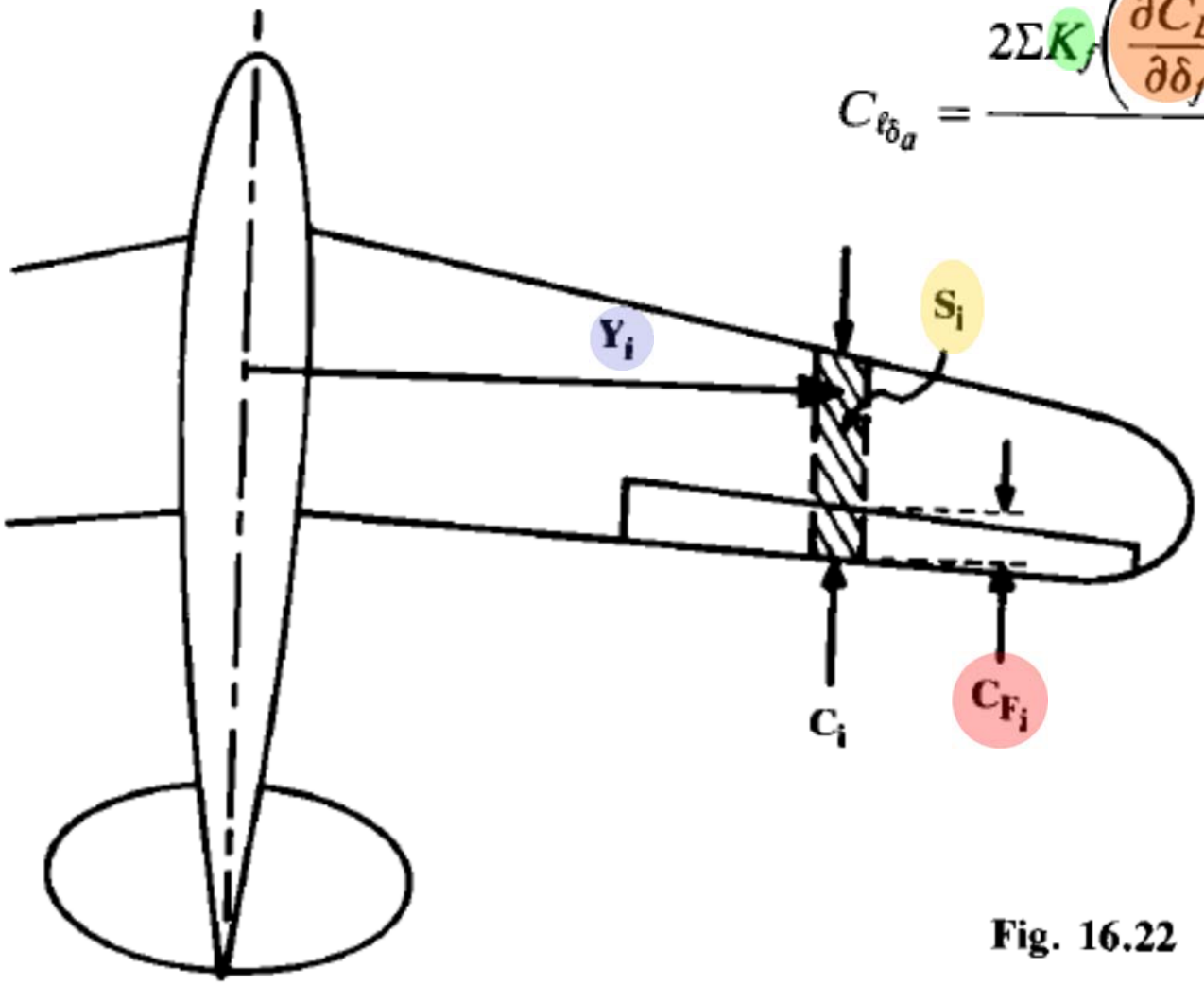

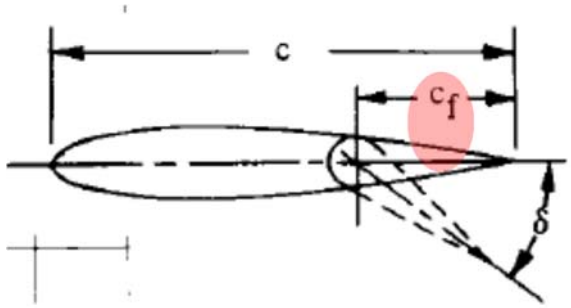

Fig. 16.22 Aileron strip geometry.

Fig A31B

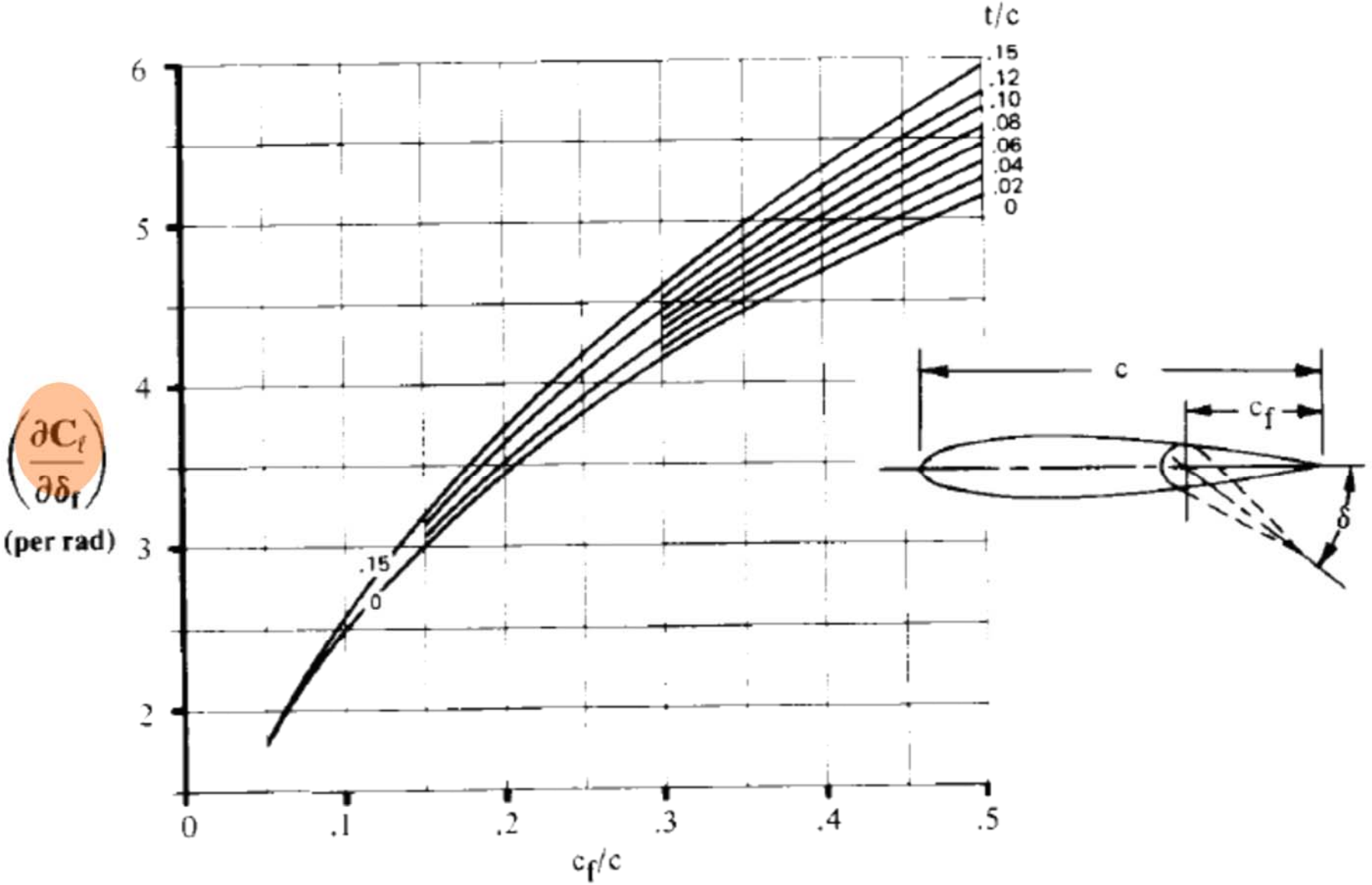

Fig. 16.6 Theoretical lift increment for plain flaps. (Ref. 37)

Fig A31C

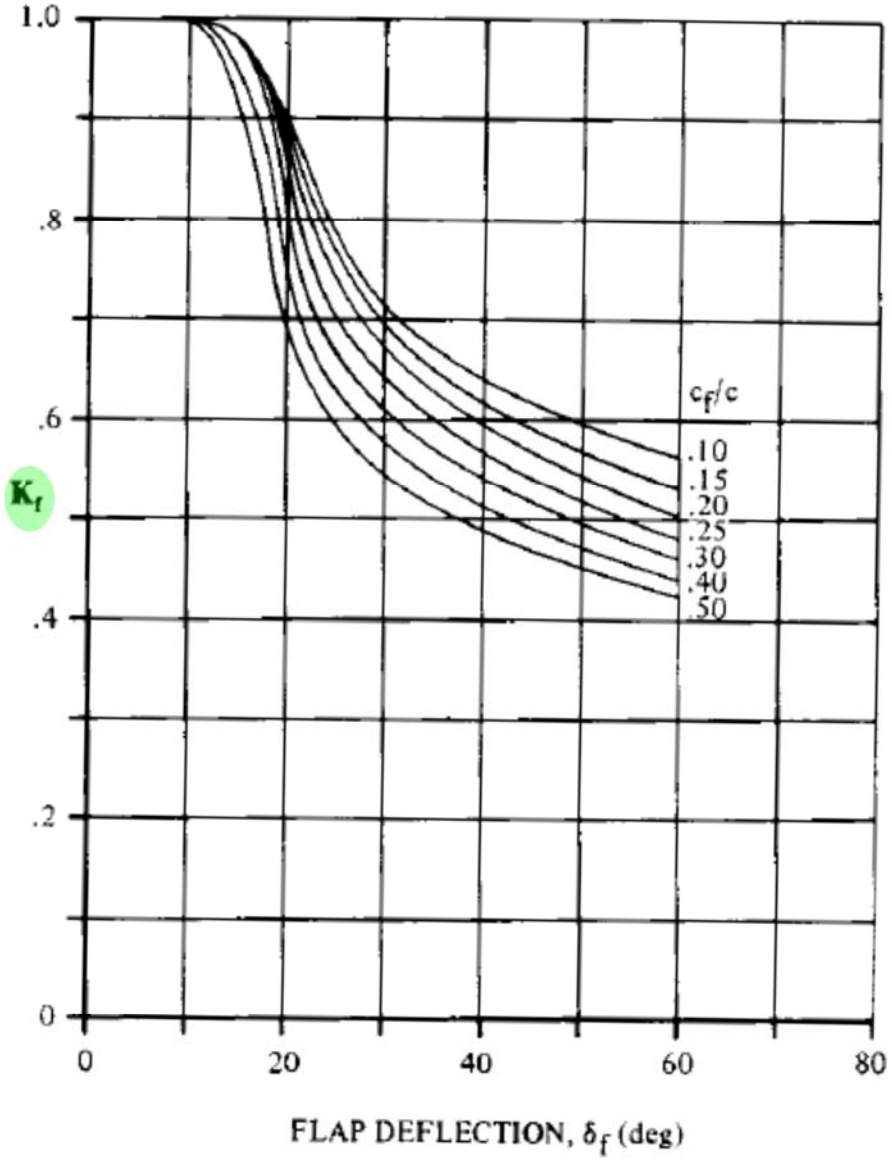

Fig. 16.7 Empirical correction for plain lift increment. (Ref. 37)

Método Genérico

Fig 31D

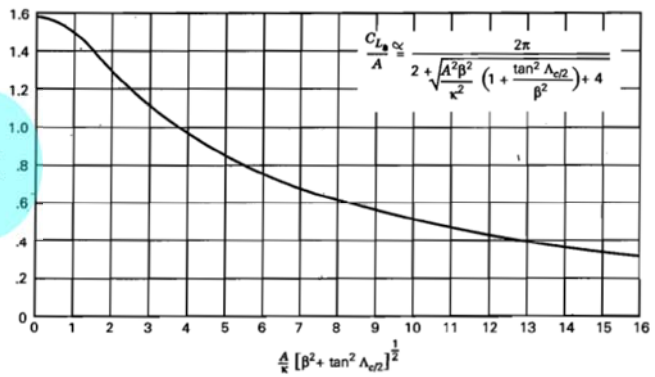

Figure B.1,2 Subsonic wing lift-curve slope.

Fig 31E

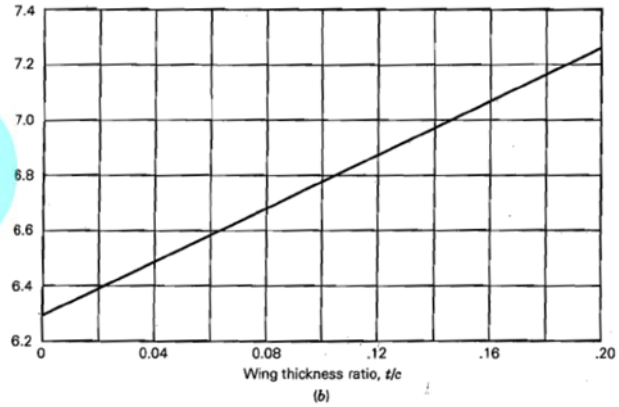

Figure B.1,1 Two-dimensional lift-curve slope.

Fig 31F

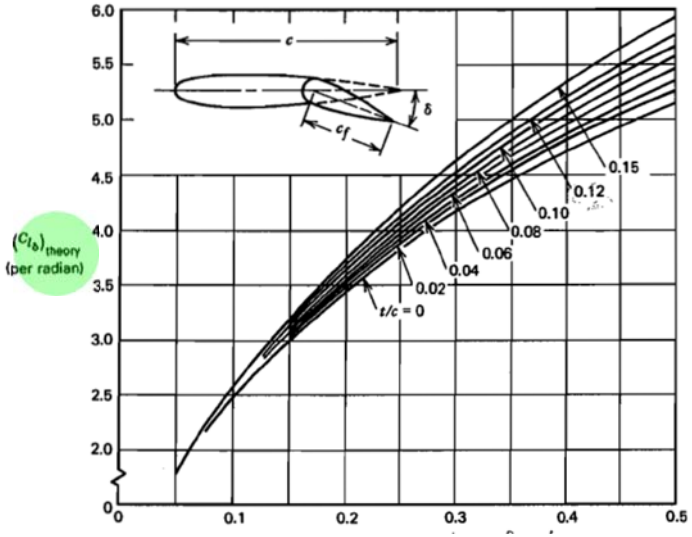

$$C_{L_\delta} = C_{l_\delta}\left(\frac{C_{L_\alpha}}{C_{l_\alpha}}\right)K_1K_2$$

Fig 31G

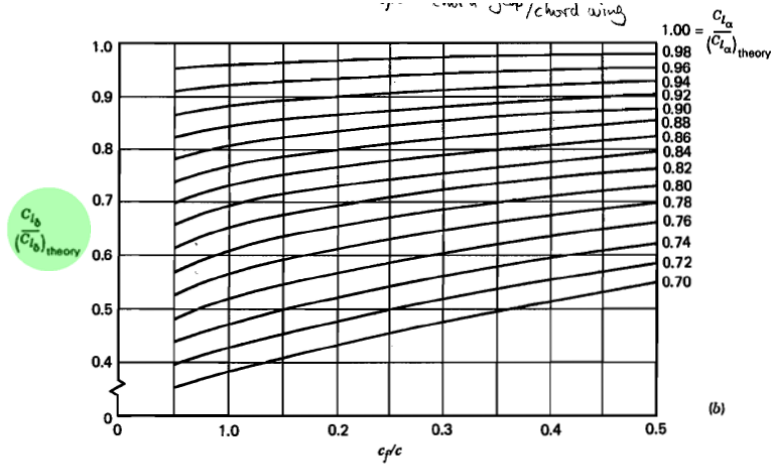

Figure B.2,1 Control effectiveness for two-dimensional incompressible flow. (From Royal Aeronautical Society Data Sheet Controls 01.01.03.)

Fig 31H

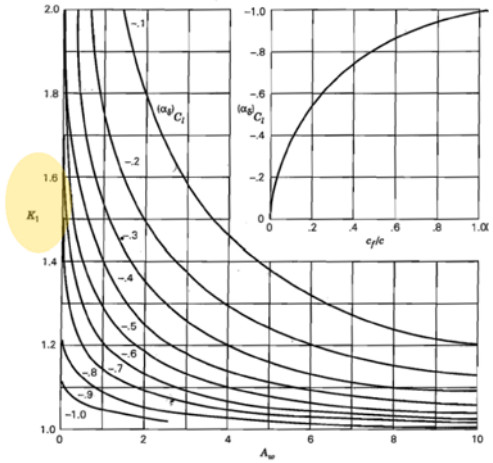

Figure B.2,2 Flap-chord factor.

Fig 31I

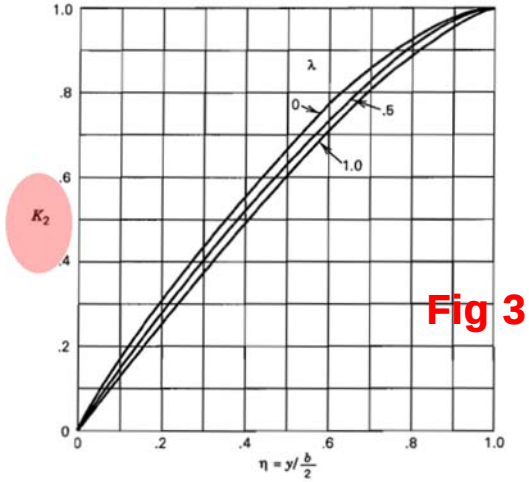

Figure B.2,3 Span factor for inboard flaps.

Fig A31D

$$C_{L_\delta} = C_{l_\delta}\left(\frac{C_{L_\alpha}}{C_{l_\alpha}}\right)K_1K_2$$

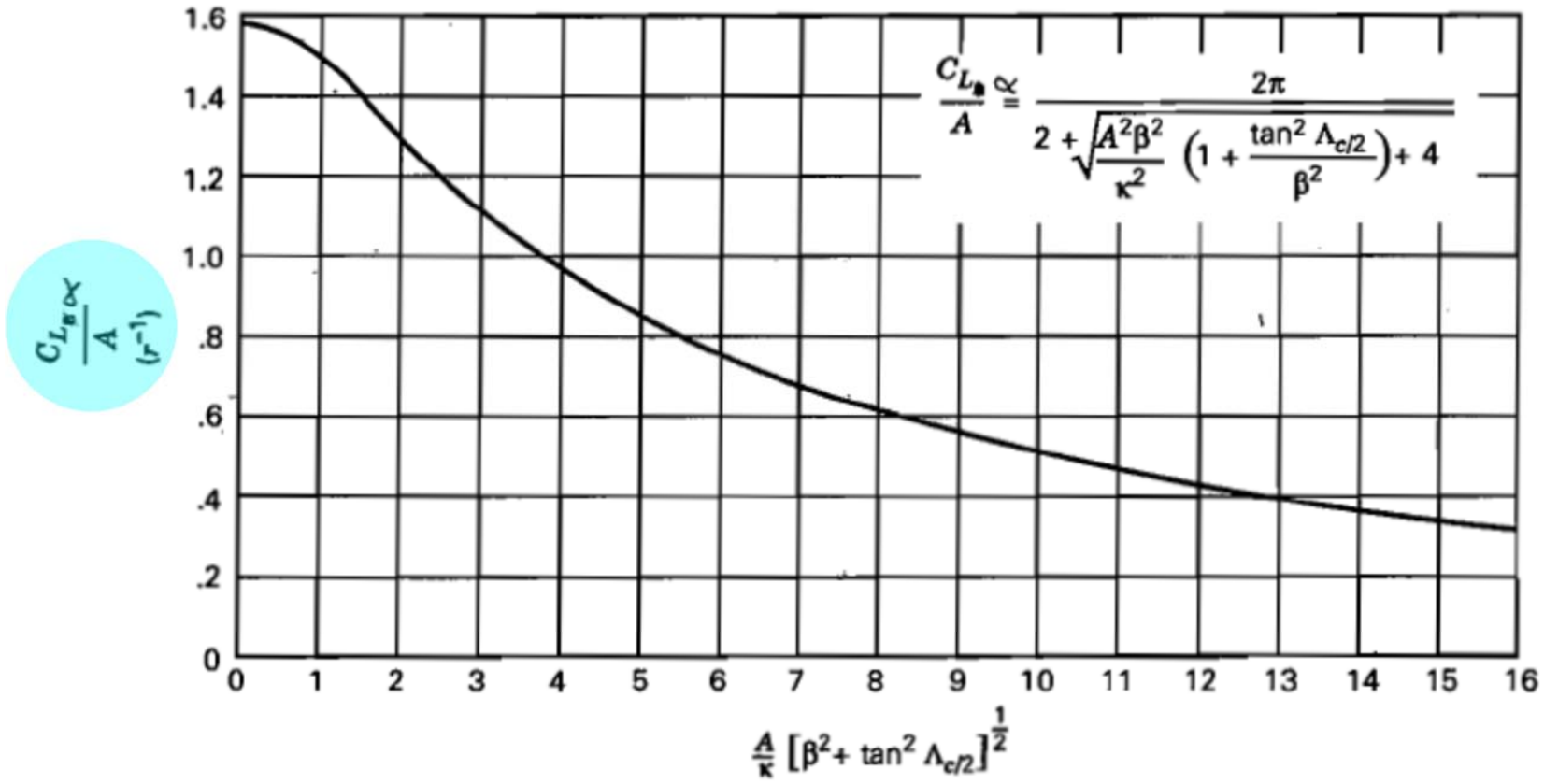

Figure B.1,2 Subsonic wing lift-curve slope.

Fig A31E

$$C_{L_\delta} = C_{l_\delta}\left(\frac{C_{L_\alpha}}{C_{l_\alpha}}\right) K_1 K_2$$

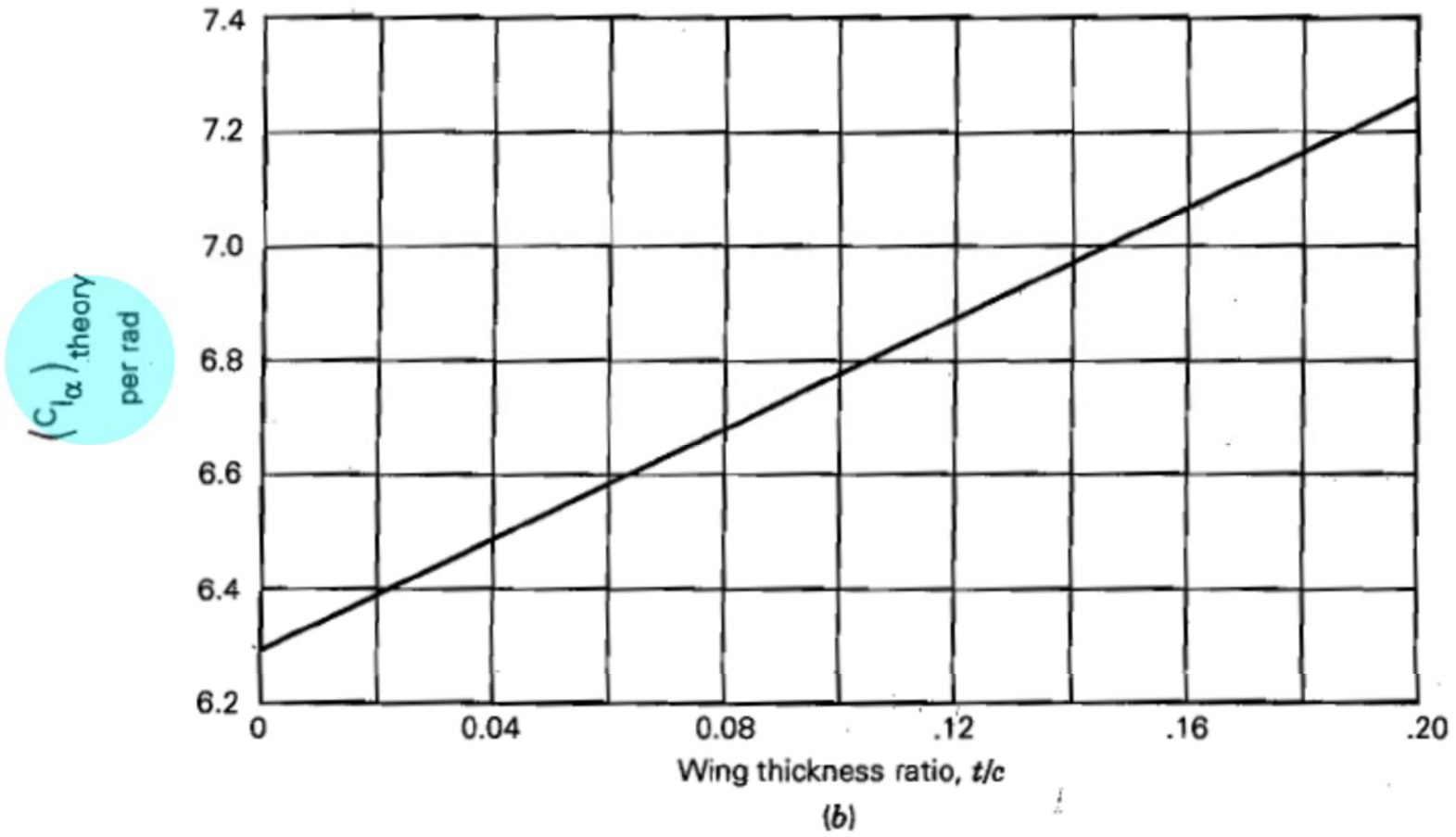

Figure B.1,1 **Two-dimensional lift-curve slope.**

Fig A31F

$$C_{L_\delta} = C_{l_\delta}\left(\frac{C_{L_\alpha}}{C_{l_\alpha}}\right)K_1 K_2$$

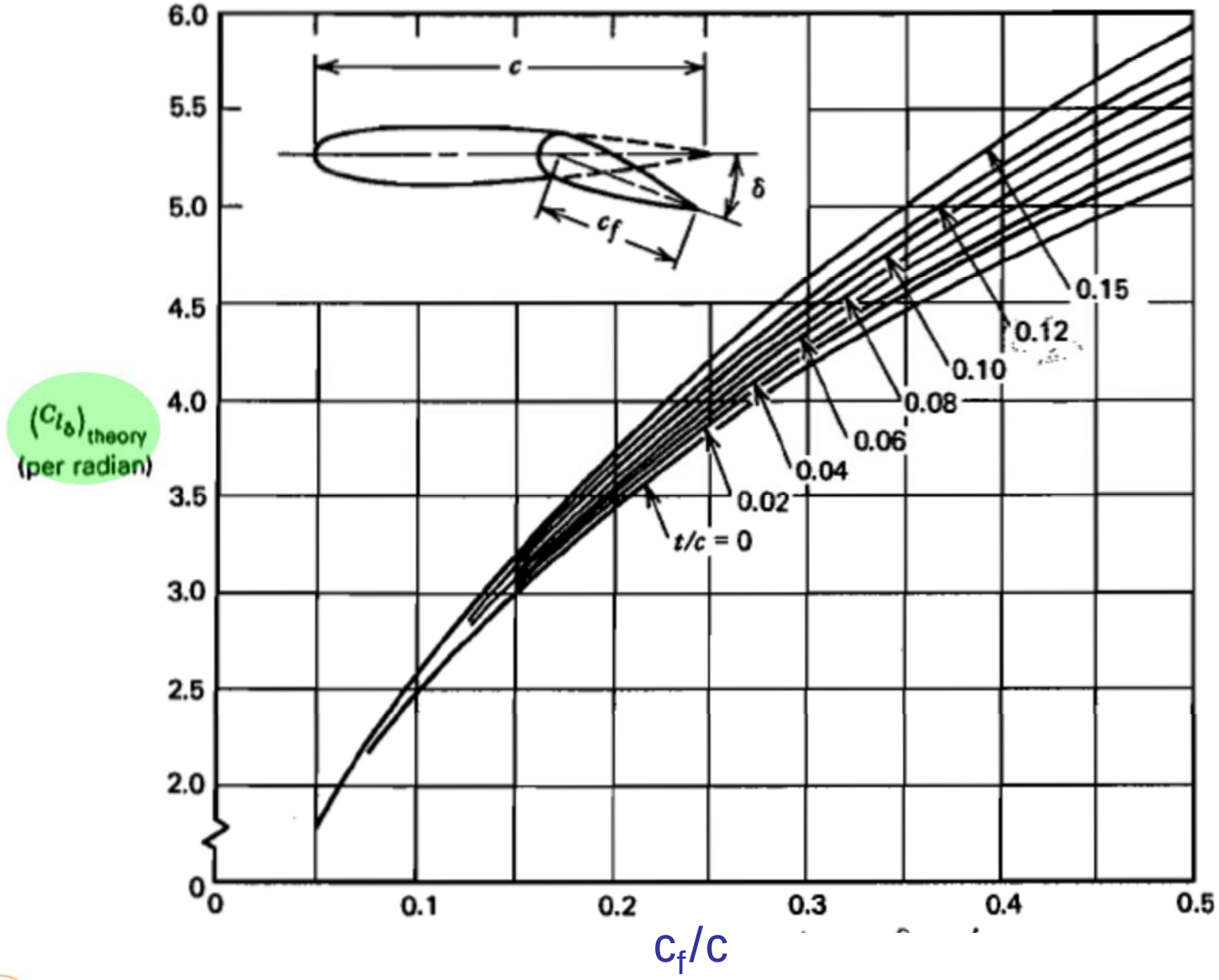

Fig A31G

$$C_{L_\delta} = C_{l_\delta}\left(\frac{C_{L_\alpha}}{C_{l_\alpha}}\right)K_1K_2$$

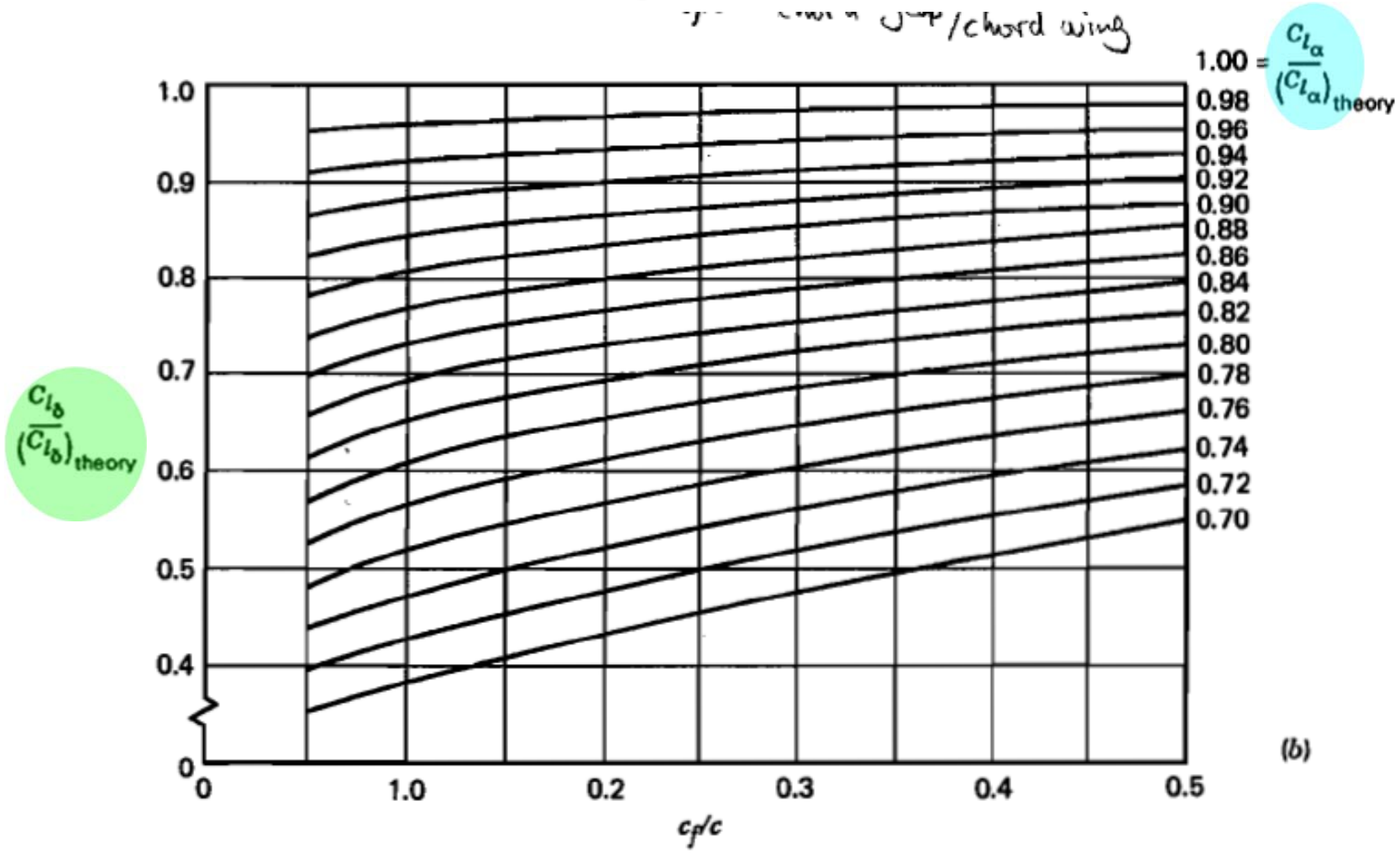

Figure B.2,1 Control effectiveness for two-dimensional incompressible flow. (From Royal Aeronautical Society Data Sheet Controls 01.01.03.)

Fig A31H

$$C_{L_\delta} = C_{l_\delta}\left(\frac{C_{L_\alpha}}{C_{l_\alpha}}\right) K_1 K_2$$

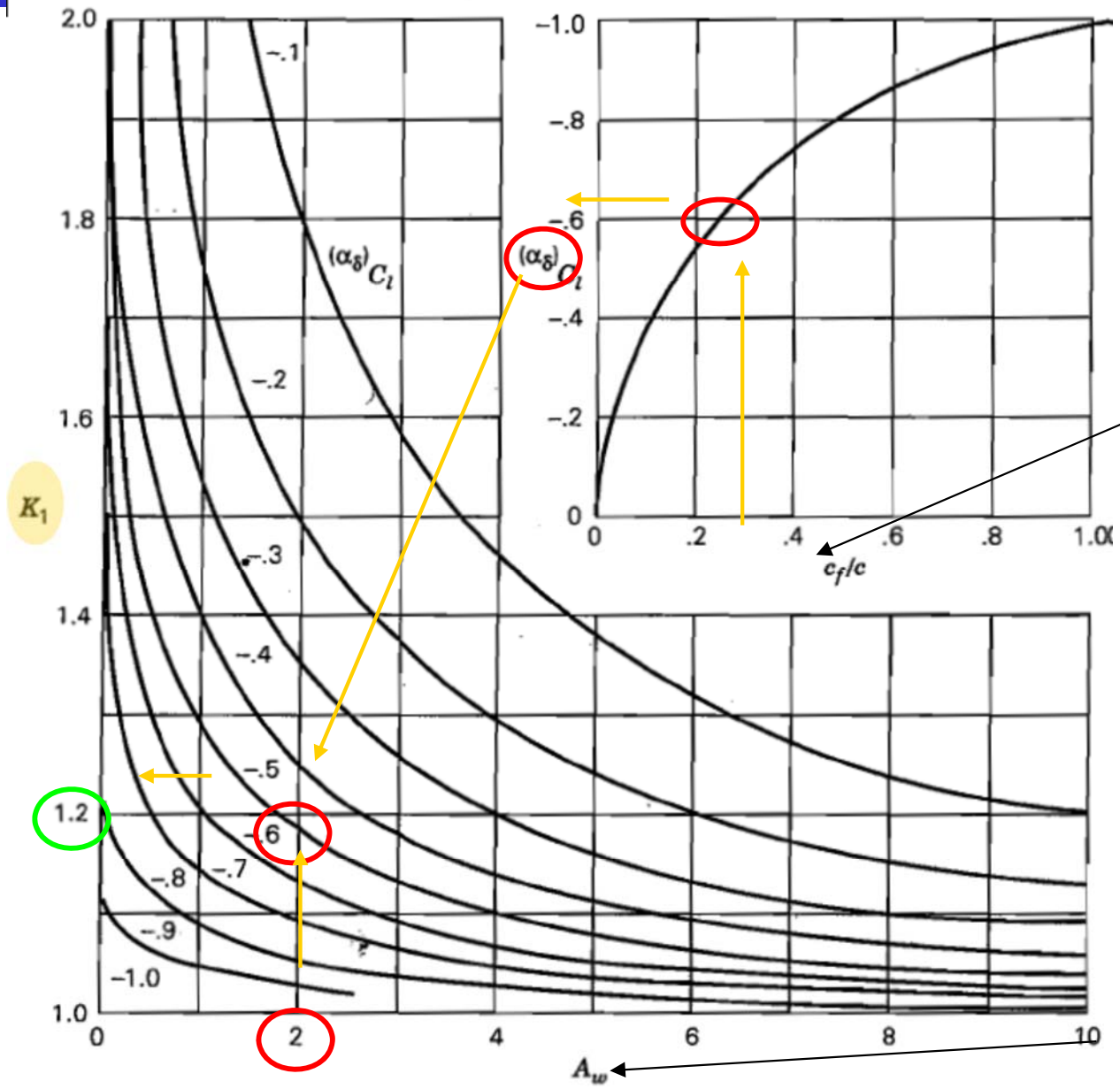

Figure B.2,2 Flap-chord factor.

Relación entre cuerdas superficie de control/ estabilizador

- Selección c_E/c_t
- Genera $(\alpha_\delta)_{Cl}$
- Selección AR_t y $(\alpha_\delta)_{Cl}$
-Genera $(\alpha_\delta)_{CL}$ $(\alpha_\delta)_{Cl}$

Alargamiento del estabilizador

Fig A31I

$$C_{L_\delta} = C_{l_\delta}\left(\frac{C_{L_\alpha}}{C_{l_\alpha}}\right) K_1 K_2$$

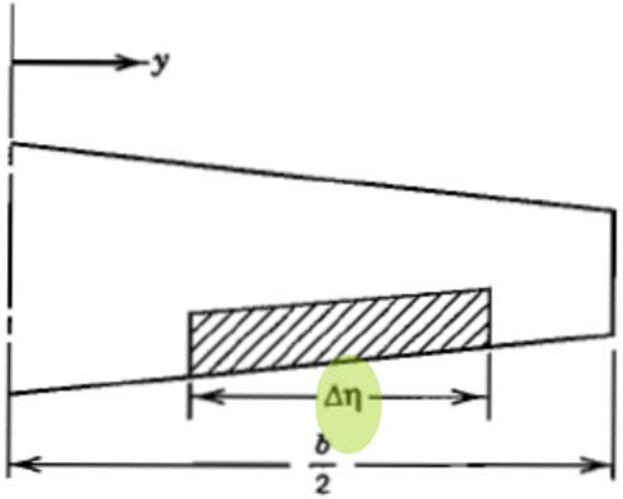

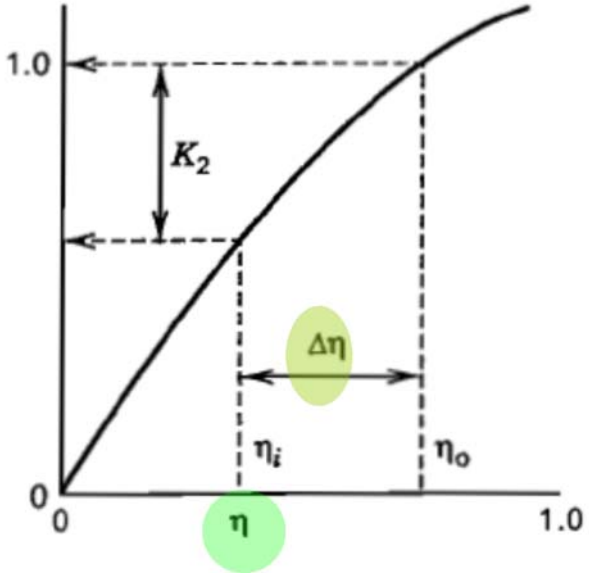

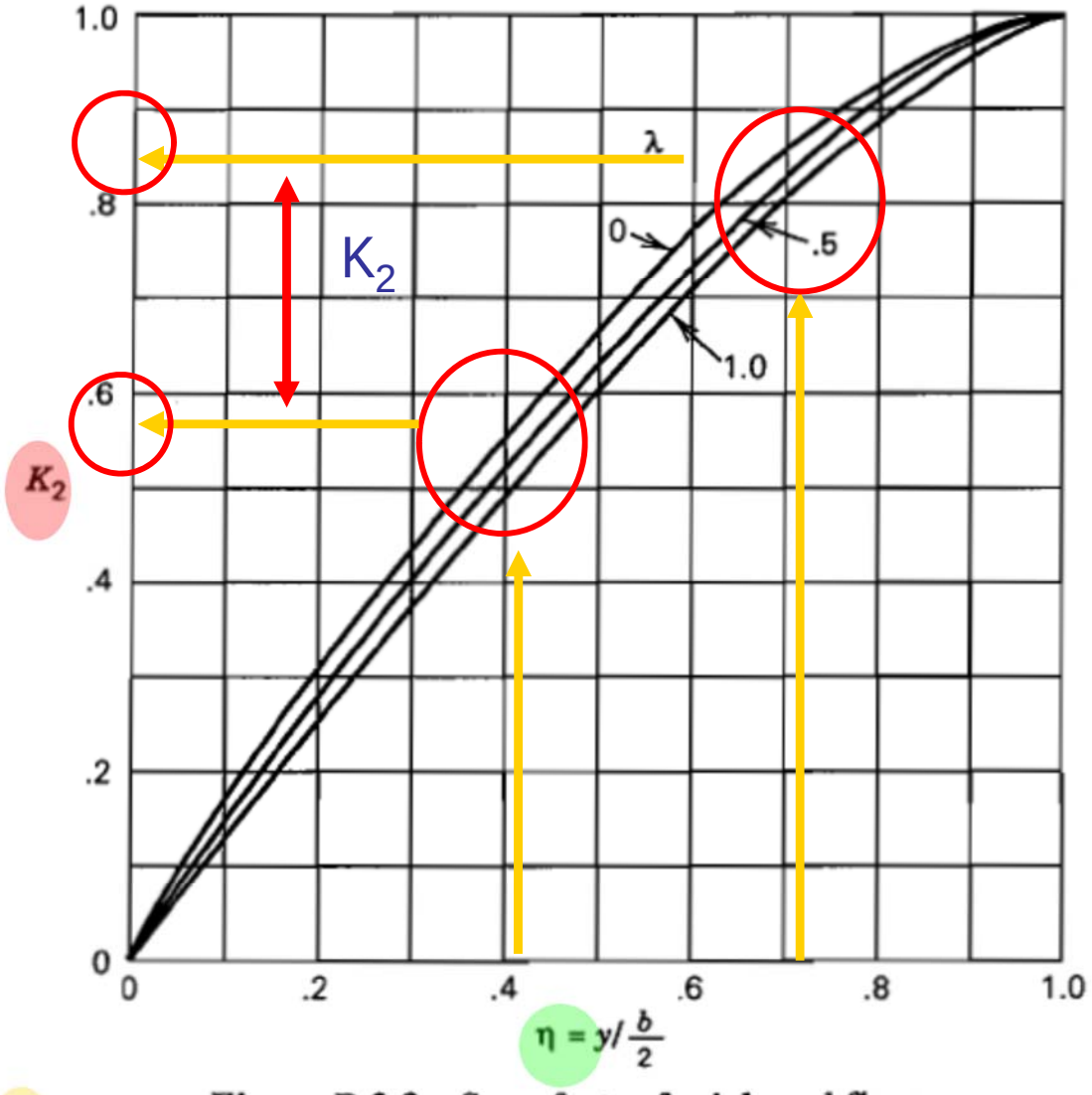

Figure B.2,3 Span factor for inboard flaps.

Control Derivatives $C_{N_{\delta_a}}$

$C_{N_{\delta_a}}$ the change in yawing moment coefficient with variation in aileron deflection

$$C_{n_{\delta_A}} = 2K C_L C_{\ell_{\delta_A}}$$

$$\eta = \frac{Y_i}{b_w/2} = \frac{\text{spanwise distance from centerline to the inboard edge of the control surface}}{\text{semispan}}$$

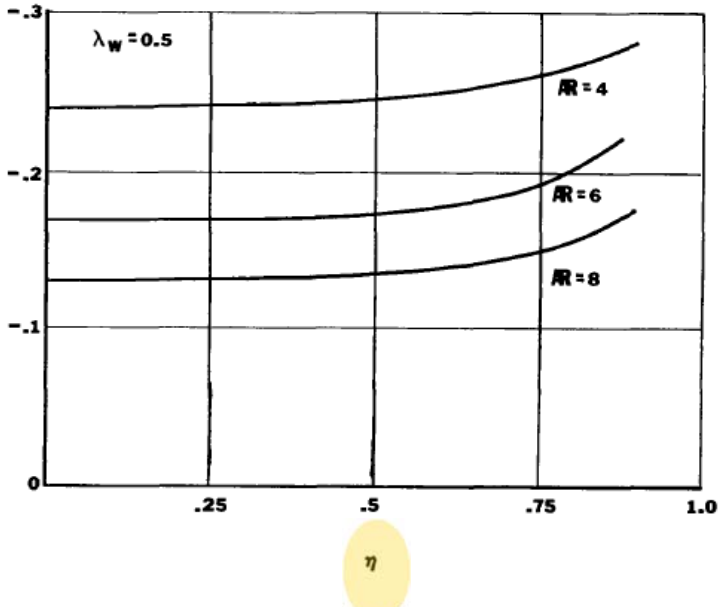

Fig A32

Figure 43. Empirical factor K as a function of η for taper ratio = 0.5.

Fig A32

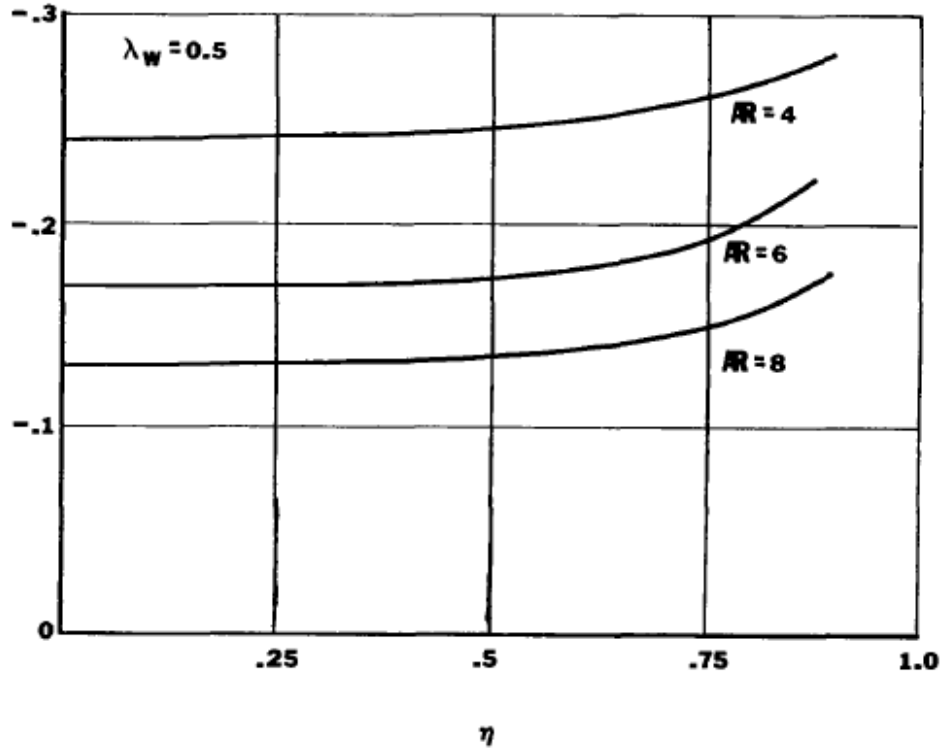

Figure 43. Empirical factor K as a function of η for taper ratio = 0.5.

$$C_{n_{\delta_A}} = 2K\, C_L\, C_{\ell_{\delta_A}}$$

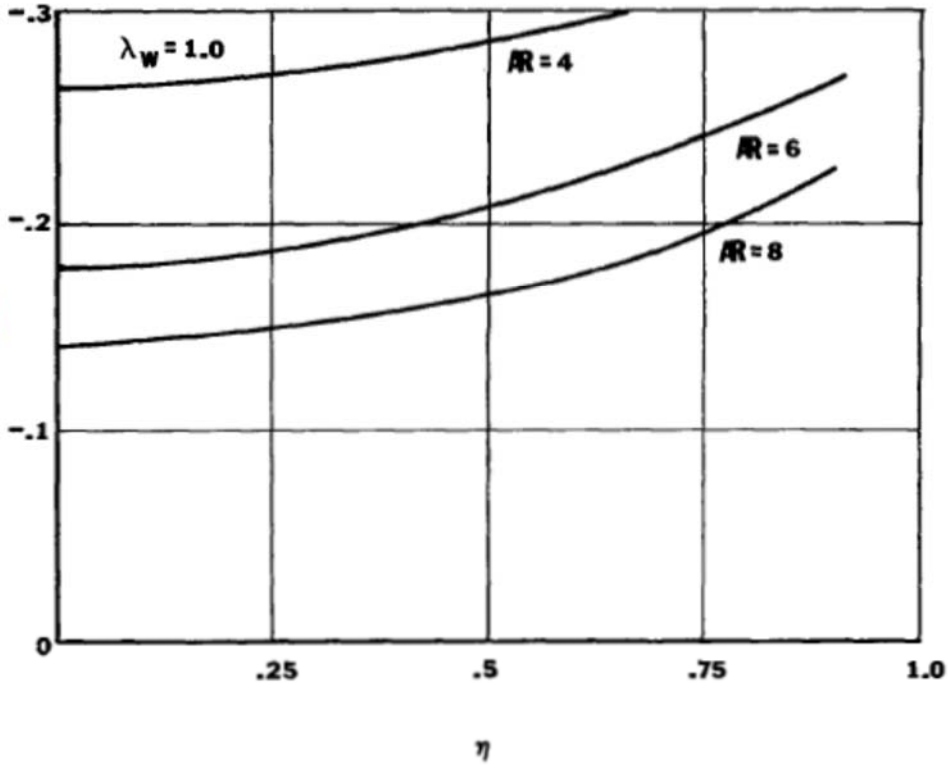

Figure 44. Empirical factor K as a function of η for taper ratio = 1.0.

Control Derivatives $C_{Y_{\delta_r}}$ $C_{L_{\delta_r}}$ $C_{N_{\delta_r}}$

$C_{Y_{\delta_r}}$ is the change in side force resulting from rudder deflection.

$$C_{y_{\delta R}} = a_v \tau \frac{S_v}{S_w}$$

a_v = lift curve slope of the vertical tail

τ = a function of rudder area to vertical tail area ratio as found from the graph below.

$C_{L_{\delta_r}}$ is the variation in rolling moment coefficient with change in rudder deflection.

$$C_{\ell_{\delta R}} = a_v \tau \frac{S_v}{S} \frac{z_v}{b_w}$$

z_v = distance from the x-axis to aerodyanmic center of the vertical tail

$C_{N_{\delta_r}}$ is the variation in yawing moment coefficient with a change in rudder deflection.

$$C_{n_{\delta R}} = - a_v \tau \frac{S_v}{S_w} \frac{\ell_v}{b_w} \eta_v$$

Fig A33

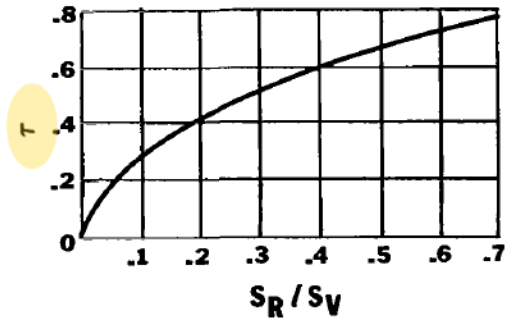

Figure 45. Values for τ as a function of rudder area to vertical tail area ratio.

Fig A33

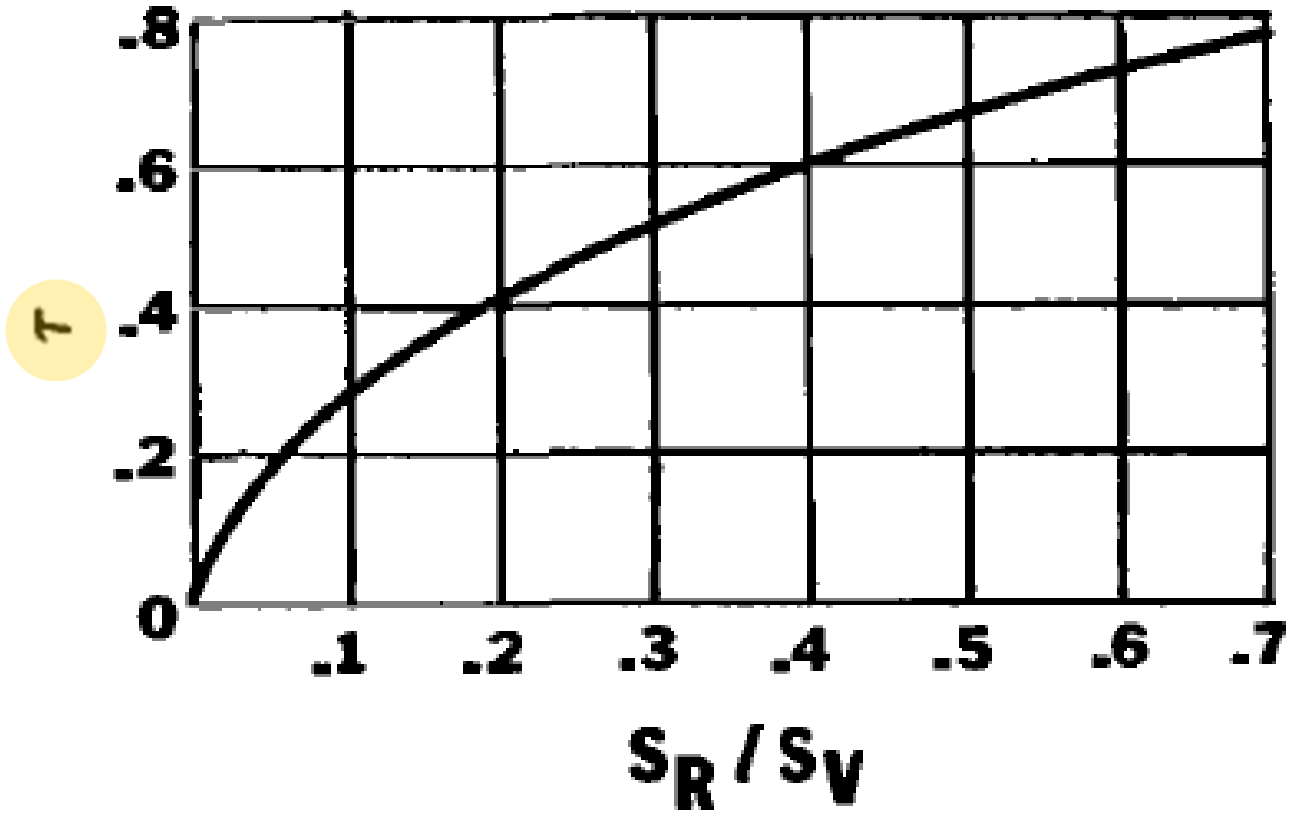

Figure 45. Values for τ as a function of rudder area to vertical tail area ratio.

Bibliografia

- Performance, Stability, Dynamics, and Control of Airplanes, Bandu N. Pamadi, AIAA Education Series.
- Riding and Handling Qualities of Light Aircraft – A Review and Analysis, Frederick O. Smetana, Delbert C. Summey, and W. Donnald Johnson, Report No. NASA CR-1975, March 1972.
- Airplane Aerodynamics and Performance, Dr. Jan Roskam and Dr. Chuan-Tau Edward Lan, DARcorporation, 1997.
- Flight Vehicle Performance and Aerodynamic Control, Frederick O. Smetana, AIAA Educaction Series, 2001.
- Dynamics of Flight: Stability and Control, Bernard Etkin and LloyidDuff Reid, John Wiley and Sons, Inc. 1996.